R. & M. No. 2947
(15,933)
A.R.C. Technical Report

MINISTRY OF SUPPLY

AERONAUTICAL RESEARCH COUNCIL
REPORTS AND MEMORANDA

The Calculation of the Loading and Pressure Distribution on Cranked Wings

By

G. G. BREBNER, M.A.

LONDON: HER MAJESTY'S STATIONERY OFFICE
1955
EIGHT SHILLINGS NET

The Calculation of the Loading and Pressure Distribution on Cranked Wings

By

G. G. BREBNER, M.A.

COMMUNICATED BY THE PRINCIPAL DIRECTOR OF SCIENTIFIC RESEARCH (AIR), MINISTRY OF SUPPLY

Reports and Memoranda No. 2947*

January, 1953

Summary.—Using distributions of vortices and sources over the aerofoil surface, approximate formulae are developed for finding the spanwise and chordwise loadings of cranked wings (*i.e.*, wings with discontinuous changes of sweep), and the chordwise pressure distribution at the crank, in incompressible flow. The method can be extended to sub-critical compressible flow by considering the ' analogous wing.' Calculations by the present method are compared with experimental results on two wings and with calculations by another method for wings of M, W and Λ plan-form. Agreement with experiment is good. Comparison with the other method shows satisfactory agreement between the spanwise loadings, but the present method yields more information about chordwise distributions, and is quicker.

1. *Introduction.*—The term 'cranked wing ' is here used to denote a wing on which the angle of sweep changes abruptly at one or more sections between the centre and the tip. These cranks are distinct from the ' kink ' at the centre-section of a swept wing, which is, indeed, a special case of a crank. Effects at the kink of a swept wing have been extensively studied (*e.g.*, Refs. 18, 19, 20), but so far those at a crank have not.

The use of cranked wings has been considered for some time, ever since swept-back wings were seen to have unsatisfactory stalling and pitching-moment characteristics and to involve structural difficulties due to elastic distortions. The typical longitudinal instability of a swept-back wing is due to flow breakdown near the tips and the comparatively long moment arm between the tips and the centre of gravity. To minimise this instability, wings have been designed on which the sweepback decreases near the tip, thereby reducing both the likelihood of flow breakdown and the length of the moment arm. Such a change of sweepback usually takes place suddenly at a crank, and up to the present has been of the order of 10 to 20 deg in practical cases. To overcome the bending moment and torsion problems while trying to preserve the benefits of sweepback, wings of M, W and Λ plan-form have been proposed. In such cases the changes of sweep at the cranks are usually greater than the 10 to 20 deg mentioned above, and may even be as large as 90 deg, or more.

Investigations into the behaviour of such wings have, in the past, been mainly experimental. No real theoretical study has been made of conditions near the crank, although some existing calculation methods for the loading distribution can be applied to wings of cranked plan-form and take account of the crank effect to a certain extent. For instance, in Refs. 1 and 2, horseshoe vortices are distributed along the quarter-chord line, and Falkner's method[3] can also be used by placing the horseshoe vortices so as to conform to the wing geometry. The first two methods

* R.A.E Report Aero. 2483, received 14th May, 1953.

give no information about the chordwise loading, however, and the third method would require a number of chordwise pivotal points, which would greatly increase the computational work involved.

The presence of the crank affects the chordwise loading in its vicinity, and hence the sectional lift slope and the spanwise loading. This report presents a method of calculating these loadings and pressure distributions. The method is based on the velocities induced in incompressible flow by distributions of source lines and vortex lines cranked to follow the wing plan-form. The calculation of the pressure distribution and loading at a crank is one of the ' basic ' solutions for a swept wing, like those for the kink and the part of the wing which acts as a sheared wing. Conditions at other sections are determined from the basic solutions by superposing the contributions from the kink, crank and sheared part. It can be seen intuitively that conditions at a crank like those shown in Fig. 2a bear some resemblance to conditions at the centre of a swept-forward wing, and therefore high suction peaks can be expected near the nose of the crank section. A means of reducing these suction peaks by the use of camber and twist is suggested. The results of the calculations are compared with experimental data at the crank of the wing shown in Fig. 2b and a double-cranked wing, and also with the results of other calculation methods for wings of complicated plan-forms.

The present report fits into the calculation scheme for wings of any planform, which was originated in Refs. 4 and 5 and recently extended in Ref. 6. The method may be extended to compressible flow below the critical Mach number by using the well-known concept of the ' analogous wing ' as described in Ref. 6. The effect of cambered sections may be dealt with by the method of Ref. 7 and wing-body combinations by the method of Ref. 8. In connection with the suggested use of cranked wings for structural reasons, it is of interest to note that Hunn[9] has recently extended the spanwise loading calculation procedure of Refs. 4 and 5 to elastic wings.

2. *The Chordwise Loading at the Crank of an Infinite Thin Wing of Symmetrical Section.*— We will deal first with the chordwise loading of a thin cranked wing of symmetrical section, and represent the lifting effect of the wing by a sheet of vortex lines distributed over the chordal plane of the wing. These lines run in a spanwise direction and are kinked and cranked to follow the wing plan-form. To isolate the effect of a crank from that of a kink or tip, we will treat initially a wing which extends to infinity on either side of a single crank : thus the vortices which represent the lifting effect of this wing extend to infinity on either side of the crank.

Consider two semi-infinite vortex filaments in the plane $z = 0$ stretching to infinity on each side of their intersection in the plane $y = 0$, as in Fig. 1a. All the vortex lines in the two filaments are of equal vorticity $\gamma(x)$, which is independent of y. The sweep angles of the filaments are φ_i and φ_o, the former being regarded as the sweep of the inboard panel of the starboard half of a cranked wing, and the latter as the sweep of the outboard panel. Both angles are regarded as positive in the directions shown in Fig. 1a. The strengths of the vortex filaments are $\gamma(x) \cos \varphi_i \, dx$ and $\gamma(x) \cos \varphi_o \, dx$, where dx is the width of the filament in the free-stream direction and $\gamma(x)$ is a function of x, the streamwise distance from the leading edge of the wing.

From equation (1) in Appendix I of Ref. 5 it can be seen that in the plane $y = 0$, *i.e.*, at the crank, the downwash velocity at a point $(x, 0, z)$ due to the left-hand filament through $(x', 0, 0)$ is

$$\left[\frac{dv_z}{V_0}\right]_i = \frac{\gamma(x')\,dx'}{4\pi V_0} \frac{x - x'}{(x - x')^2 + \dfrac{z^2}{\cos^2 \varphi_i}} \left\{1 - \sin \varphi_i \frac{x - x'}{\sqrt{[(x - x')^2 + z^2]}}\right\} \quad .. \quad (1)$$

and the downwash due to the right-hand filament is

$$\left[\frac{dv_z}{V_0}\right]_o = \frac{\gamma(x')\,dx'}{4\pi V_0} \frac{x - x'}{(x - x')^2 + \dfrac{z^2}{\cos^2 \varphi_o}} \left\{1 + \sin \varphi_o \cdot \frac{x - x'}{\sqrt{[(x - x')^2 + z^2]}}\right\} . \quad .. \quad (2)$$

If we now consider the lifting effect of a thin infinite cranked wing of symmetrical section as being represented by a continuous chordwise distribution of such vortex filaments $\gamma(x')$, (x' being the current co-ordinate), in the range $0 \leqslant x' \leqslant 1$, then the downwash at a point $(x, 0, 0)$ on the crank section ($0 \leqslant x \leqslant 1$) is obtained by integrating equations (1) and (2) over the chord and putting $z = 0$. That is, the downwash at the crank is half of that at the kink of a swept-forward wing ($\varphi = \varphi_i$) plus half of that at the kink of a swept-back wing ($\varphi = \varphi_o$).

For an infinite kinked vortex distribution, as in Ref. 5, the downwash in the plane $y = 0$ is

$$\frac{v_z(x, 0, z)}{V_0} = \frac{1}{2\pi V_0}\{I_1(x, 0, z) + I_2(x, 0, z) + I_3(x, 0, z)\} \quad .. \quad .. \quad .. \quad (3)$$

where

$$I_1 = \int_0^1 \gamma(x') \frac{x - x'}{(x - x')^2 + \dfrac{z^2}{\cos^2\varphi}}\, dx'$$

$$I_2 = \sin\varphi \int_0^1 \gamma(x') \frac{dx'}{\sqrt{[(x - x')^2 + z^2]}}$$

and

$$I_3 = -\sin\varphi \int_0^1 \gamma(x') \frac{\dfrac{z^2}{\cos^2\varphi}}{\left\{(x - x')^2 + \dfrac{z^2}{\cos^2\varphi}\right\}\sqrt{[(x - x')^2 + z^2]}}\, dx'.$$

Since we are dealing with a representation of a thin wing, these integrals are evaluated for $z \to 0$. If this proves impracticable, however, they may be evaluated for $z \neq 0$, since the assumption of a thin wing is meant to be a simplification, not a complication. I_1 is the ordinary downwash integral for a two-dimensional aerofoil and can be evaluated at $z = 0$. I_2 has a logarithmic infinity on the x-axis and calculating it for non-zero values of z reveals that within the practical range of thickness/chord ratios it is not very sensitive to the value of t/c or of x. Thus a mean value can be used for the practical range of thickness/chord ratios. For a given wing, $I_2 =$ constant $\times\ \gamma(x)$. The integrand of I_3 has an infinity at the point $(x, 0, 0)$, the appropriate value of I_3 being the principal value. This, too is proportional to $\gamma(x)$. Equation (3) then becomes

$$\frac{v_z}{V_0} = \frac{1}{2\pi V_0}\left\{\int_0^1 \gamma(x') \frac{dx'}{x - x'} + \pi \tan\varphi \,.\, \gamma(x)\right\}, \quad .. \quad .. \quad .. \quad .. \quad (4)$$

the second term comprising I_2 and I_3.

Therefore for the left-hand distribution of semi-infinite swept vortex filaments, the downwash at the point $(x, 0, 0)$ is given by the approximation

$$\left[\frac{v_z}{V_0}\right]_i = \frac{1}{4\pi V_0}\left\{\int_0^1 \gamma(x') \frac{dx'}{x - x'} - \pi \tan\varphi_i \,.\, \gamma(x)\right\}$$

and the downwash due to the right-hand distribution of vortex filaments is

$$\left[\frac{v_z}{V_0}\right]_o = \frac{1}{4\pi V_0}\left\{\int_0^1 \gamma(x') \frac{dx'}{x - x'} + \pi \tan\varphi_0 \,.\, \gamma(x)\right\}.$$

Therefore the total downwash at the point $(x, 0, 0)$ is

$$\frac{v_z}{V_0} = \frac{1}{2\pi V_0}\left\{\int_0^1 \gamma(x')\frac{dx'}{x-x'} + \pi\frac{\tan\varphi_o - \tan\varphi_i}{2}\gamma(x)\right\}$$

$$= \frac{1}{2\pi V_0}\left\{\int_0^1 \gamma(x')\frac{dx'}{x-x'} + \pi\tan\varphi^*.\gamma(x),\right\}, \quad .. \quad .. \quad .. \quad .. \quad (5)$$

where

$$\tan\varphi^* = \frac{\tan\varphi_o - \tan\varphi_i}{2} \quad .. \quad .. \quad .. \quad .. \quad .. \quad .. \quad .. \quad (6)$$

defines φ^*. φ^* has no geometrical significance: it is a measure of the 'crank effect,' which equation (5) shows to be like that at the kink of a wing swept at an angle φ^*.

As in Küchemann's reports on wing loading[5, 6], $\gamma(x)$ is assumed to be of the form $C\{(1-x)/x\}^n$, where C is independent of x. If v_z/V_0 is constant over the chord and equal to the effective incidence α_{e0}, then a solution of equation (5) is

$$\gamma(x) = 2V_0\,\alpha_{e0}\sin\pi n_0^*\left(\frac{1-x}{x}\right)^{n_0^*} \quad .. \quad .. \quad .. \quad .. \quad .. \quad (7)$$

where n_0^* is the value of n at the crank of the infinite wing. (The suffix $_0$ applied to α_e and n denotes the infinite wing.)

Combining equations (5) and (7),

$$\frac{v_z}{V_0} = \alpha_{e0} = \frac{2V_0\alpha_{e0}\sin\pi n_0^*}{2\pi V_0}\left\{\frac{\pi}{\sin\pi n_0^*} - \left(\frac{\pi}{\tan\pi n_0^*} - \pi\tan\varphi^*\right)\left(\frac{1-x}{x}\right)^{n_0^*}\right\}$$

which is to be independent of x. Therefore

$$\tan\varphi^* = \cot\pi n_0^* = \tan\left(\frac{\pi}{2} - \pi n_0^*\right),$$

i.e.,

$$n_0^* = \tfrac{1}{2} - \frac{\varphi^*}{\pi} = \frac{1}{2}\left(1 - \frac{\varphi^*}{\pi/2}\right). \quad .. \quad .. \quad .. \quad .. \quad .. \quad .. \quad (8)$$

The kink of an infinite swept wing corresponds to the case $\varphi_i = -\varphi_o = \varphi$, and n_0^* becomes

$$n_0 = \frac{1}{2}\left(1 - \frac{\varphi}{\pi/2}\right),$$

the result obtained in Ref. 5.

The infinite sheared wing corresponds to the case $\varphi_i = \varphi_o$, and n_0^* becomes

$$n_0 = \tfrac{1}{2},$$

the 'flat-plate distribution' parameter for a two-dimensional wing.

The term containing x varies from $\{(1-x)/x\}^{n_0^*}$ at the crank to $\{(1-x)/x\}^{1/2}$ far away from the crank. In practice, this distribution is usually reached at a distance of about one chord from the crank. As shown in Ref. 5, the chordwise position of the aerodynamic centre, measured from the quarter-chord point, is

$$\Delta x_{\text{a.c.}} = x_{\text{a.c.}} - \frac{1}{4} = \frac{1-2n}{4},$$

where n is the index in the function of x. It is reasonable to assume that the aerodynamic centre changes continuously from its position at the sheared wing to its position at the crank, and thus that the chordwise vorticity distributions at intermediate points have the one-parameter form of equation (7), with n varying continuously. At such an intermediate point we can write

$$\frac{1-2n}{4} = \Delta x_{\text{a.c.}} = \lambda[\Delta x_{\text{a.c.}}]_{\text{cr.}} = \lambda\left(\frac{1-2n_0^*}{4}\right),$$

where $0 \leqslant \lambda \leqslant 1$ and λ depends on the spanwise distance from the crank : i.e., $\lambda = \lambda(y)$. $\lambda = 1$ at the crank and 0 at the sheared part. The intermediate value of n is then given by

$$n = \frac{1-\lambda(1-2n_0^*)}{2} = \frac{1-\lambda+\lambda-\lambda\dfrac{\varphi^*}{\pi/2}}{2}$$

$$= \frac{1}{2}\left(1-\lambda\frac{\varphi^*}{\pi/2}\right).$$

As for the dependence of λ on y, it is assumed that the same functional relationship as has been derived for the special case of the kink still holds. $\lambda(y)$ may be obtained from Fig. 1 of Ref. 5, Fig. 1 of Ref. 7 or Fig. 23 of Ref. 6, in which $\lambda(y)$ is plotted against y (dimensionless with the local chord at the spanwise position concerned) ; or from the formula[6] :

$$\lambda(y) = 1{\cdot}40 + 1{\cdot}33y - \sqrt{(0{\cdot}16 + 7{\cdot}30y)} \quad . \quad . \quad . \quad . \quad . \quad . \quad (9)$$

λ measured from the crank section will be called $\lambda_{\text{cr.}}$. If $\varphi_i < \varphi_o$, the crank effect is like that of the kink of a swept-back wing and $\lambda_{\text{cr.}}\,\varphi^* > 0$. If $\varphi_i > \varphi_o$ the crank effect is like that of the kink of a swept-forward wing and $\lambda_{\text{cr.}}\,\varphi^* < 0$. From now on the definition of n_0 and n_0^* will be extended as follows :

$$n_0 = \frac{1}{2}\left(1-\lambda\frac{\varphi}{\pi/2}\right),$$

where λ is measured from the centre of an infinite swept wing of sweep angle φ :

$$n_0^* = \frac{1}{2}\left(1-\lambda_{\text{cr.}}\frac{\varphi^*}{\pi/2}\right)$$

where $\lambda_{\text{cr.}}$ is measured from the crank of an infinite cranked wing of sweep angles φ_i and φ_o such that $\tan\varphi^* = \frac{1}{2}(\tan\varphi_o - \tan\varphi_i)$. At a section near the crank $\gamma(x)$ may still be obtained from equation (7) if n_0^* has the value given above

$$n_0^* = \frac{1}{2}\left(1-\lambda_{\text{cr.}}\frac{\varphi^*}{\pi/2}\right).$$

The chordwise vortex distribution is now known in the neighbourhood of the crank, but the chordwise loading, $\Delta C_p(x)$, is not yet determined. The general relation between $\gamma(x)$ and $\Delta C_p(x)$ is

$$\Delta C_p(x) = -2\frac{\gamma(x)}{V_0}\cos\varphi_V, \quad . \quad . \quad . \quad . \quad . \quad . \quad . \quad . \quad (10)$$

where φ_V is the sweep of the vorticity vector at the point x. The value of φ_V depends mainly on the spanwise co-ordinate y, and also to some extent on the chordwise co-ordinate x. In practice it is necessary to simplify matters by taking a mean value of φ_V over the chord. This is the same simplification as has been used in Ref. 6 for swept wings without cranks, where it was found to be adequate.

If the aerodynamic centre changes continuously from the sheared wing position to the position at the crank and back again, the vorticity vectors will also curve round with a continuous change of sweep in the neighbourhood of the crank. At the crank itself they will have turned through about half the difference between φ_i and φ_o : *i.e.*, the sweep of the vorticity vectors at the crank may be approximated by :

$$[\varphi_V]_{\text{cr.}} = \frac{\varphi_i + \varphi_o}{2}. \qquad \ldots \ldots \ldots \ldots \ldots \ldots \ldots \ldots \quad (11)$$

Any errors involved in this assumption will be small and certainly less than those introduced by taking a mean value of φ_V over the chord.

This picture of curved vorticity vectors appears to conflict with the model of cranked vortex lines previously considered. We may continue to use the latter, however, by resolving the vorticity vector at any point into a component parallel to the line of sweep and a component in the chordwise direction. The latter will not contribute towards producing the lift force. The component parallel to the line of sweep will not have vorticity $\gamma(x)$ but the value

$$\left.\begin{aligned} \gamma_i(x) &= \frac{\cos\varphi_V}{\cos\varphi_i}\gamma(x) \\ \text{on the inboard part, and} & \\ \gamma_o(x) &= \frac{\cos\varphi_V}{\cos\varphi_o}\gamma(x) \end{aligned}\right\} \quad \ldots \ldots \ldots \ldots \ldots \ldots \ldots \ldots \quad (12)$$

on the outboard part. Thus if we retain the concept of cranked vortex lines, their vorticity must be allowed to vary from $\gamma(x)$ on the sheared part to another value at the crank. On approaching the crank from the inboard side

$$\gamma_i(x) = \frac{\cos\dfrac{\varphi_i + \varphi_o}{2}}{\cos\varphi_i}\gamma(x)$$

and from the outboard side

$$\gamma_o(x) = \frac{\cos\dfrac{\varphi_i + \varphi_o}{2}}{\cos\varphi_o}\gamma(x).$$

This means that not only does the vorticity component in the sweep direction, *i.e.*, the vorticity of the ' cranked vortex lines,' change gradually between the sheared part and the crank, but there is also a jump discontinuity at the crank itself. There is however no discontinuity in the chordwise loading—a physically real quantity. From the inboard side, the value of $\Delta C_p(x)$ at the crank is

$$\begin{aligned} \Delta C_p(x) &= -2\frac{\gamma_i(x)}{V_0}\cos\varphi_i \\ &= -2\frac{\gamma(x)}{V_0}\cos[\varphi_V]_{\text{cr.}} && \text{from equation (12)} \\ &= -2\frac{\gamma_o(x)}{V_0}\cos\varphi_o && \text{from equation (12)} \\ &= \Delta C_p(x) && \text{from the outboard side.} \end{aligned}$$

There is one quantity in each of these expressions for $\Delta C_p(x)$ which is not determined, namely $\gamma_i(x)$, $\gamma_o(x)$ and $\cos[\varphi_V]_{cr.}$. We must assume a value for one of them. Equation (11) gives a better approximation to $[\varphi_V]_{cr.}$ than we can get for $\gamma_i(x)$ or $\gamma_o(x)$, and so we use the expression :—

$$\Delta C_p(x) = -2\frac{\gamma(x)}{V_0}\cos\frac{\varphi_i+\varphi_o}{2} \qquad (13)$$

$$= -4\alpha_{e0}\sin\pi n_0^*\cdot\cos\frac{\varphi_i+\varphi_o}{2}\left(\frac{1-x}{x}\right)^{n_0^*} \qquad (14)$$

This can be interpreted roughly as the loading at the kink of a wing swept at an angle φ^* and yawed at an angle $\frac{1}{2}(\varphi_i+\varphi_o)$.

The sectional lift coefficient at the crank is :

$$C_L = -\int_0^1 \Delta C_p(x)\,dx = 4\alpha_{e0}\pi n_0^*\cos\frac{\varphi_i+\varphi_o}{2}$$

$$= 2a_0 n_0^*\alpha_{e0}\cos\frac{\varphi_i+\varphi_o}{2},$$

on putting $2\pi = a_0$, the lift slope of a thin two-dimensional wing. Therefore the sectional lift slope at the crank C_L/α_{e0}, is

$$a_{cr.} = 2a_0 n_0^*\cos\frac{\varphi_i+\varphi_o}{2}.$$

At distances greater than about one chord from the crank (i.e., $\lambda_{cr.} = 0$), sheared wing conditions obtain, and

$$\Delta C_p(x) = -4\alpha_{e0}\cos\varphi\left(\frac{1-x}{x}\right)^{1/2}$$

$$C_L = a_0.\alpha_{e0}\cos\varphi$$

and

$$a = a_0\cos\varphi,$$

where $\varphi = \varphi_i$ or φ_o depending on which wing panel is being considered.

At intermediate positions between crank and sheared part, the expressions for $\Delta C_p(x)$, C_L and a must contain a suitable interpolation factor to take account of the change in φ_V. This factor is

$$\frac{\cos\left[\lambda_{cr.}\dfrac{\varphi_i+\varphi_o}{2}\right]}{\cos[\lambda_{cr.}\varphi]},$$

where $\varphi = \varphi_i$ or φ_o depending on the wing panel. This factor is consistent with equation (12) and with the sheared wing and crank expressions. Then :

$$\Delta C_p(x) = -4\alpha_{e0}\sin\pi n_0^*\cos\varphi\,\frac{\cos\left[\lambda_{cr.}\dfrac{\varphi_i+\varphi_o}{2}\right]}{\cos[\lambda_{cr.}\varphi]}\left(\frac{1-x}{x}\right)^{n_0^*}$$

$$C_L = 2a_0 n_0^*\alpha_{e0}\cos\varphi\,\frac{\cos\left[\lambda_{cr.}\dfrac{\varphi_i+\varphi_o}{2}\right]}{\cos[\lambda_{cr.}\varphi]}$$

$$a = 2a_0 n_0^*\cos\varphi\,\frac{\cos\left[\lambda_{cr.}\dfrac{\varphi_i+\varphi_o}{2}\right]}{\cos[\lambda_{cr.}\varphi]}$$

are general equations applying to any spanwise position on an infinite cranked wing. The t erm $\cos\varphi \cos\left[\lambda_{cr.}\frac{\varphi_i+\varphi_o}{2}\right]\Big/\cos\left[\lambda_{cr.}\varphi\right]$ is equal to $\cos\varphi_V$, the cosine of the mean sweep of the vorticity vectors. At the crank, $\lambda_{cr.}=1$ and $\cos\varphi_V=\cos\frac{1}{2}(\varphi_i+\varphi_o)$ as was assumed in equation (11). Far from the crank on either side, $\lambda_{cr.}=0$ and $\cos\varphi_V=\cos\varphi$ where φ has the value appropriate to the wing panel concerned. The case of a finite cranked wing will be dealt with in section 5.

3. *The Chordwise Pressure Distribution at the Crank of an Infinite Thick Wing of Symmetrical Section at Zero Lift.*—We will now deal with the pressure distribution at the crank of a thick wing at zero lift. The effect of the wing thickness is represented by a distribution of source lines cranked to follow the wing plan-form. As in section 2, the crank effect is isolated by treating a wing which stretches to infinity on each side of the crank.

Consider two distributions of semi-infinite source lines in the plane $z=0$, joined at the crank like the vortex filaments of section 2. Let $q(x)$ represent the strength per unit area of such an elementary source line, so that the source strength per unit length is $q_i(x)\cos\varphi_i\,dx$ and $q_o(x)\cos\varphi_o\,dx$ for the inboard and outboard panels respectively. In the notation of Appendix I of Ref. 10, $E=q(x)\cos\varphi\,dx$. From the expressions given in that report for the velocities induced by a swept source line, the velocities induced in the x and y directions at the point $(x,\,0,\,z)$ by one such semi-infinite source line through the point $(x',\,0,\,0)$ may be written down :

$$\frac{dv_x}{V_0}=\frac{q(x')\cos\varphi\,dx'}{4\pi V_0}\,\frac{(x-x')\sqrt{[(x-x')^2+z^2]}-\dfrac{\sin\varphi}{\cos^2\varphi}z^2}{\left[(x-x')^2+\dfrac{z^2}{\cos^2\varphi}\right]\sqrt{[(x-x')^2+z^2]}}$$

and

$$\frac{dv_y}{V_0}=\frac{q(x')\cos\varphi\,dx'}{4\pi V_0}\,\frac{-(x-x')\left[\tan\varphi\sqrt{[(x-x')^2+z^2]}+\dfrac{x-x'}{\cos\varphi}\right]-\dfrac{z^2}{\cos\varphi}}{\left[(x-x')^2+\dfrac{z^2}{\cos^2\varphi}\right]\sqrt{[(x-x')^2+z^2]}}.$$

These expressions can be integrated with respect to x' over the chord to give the induced velocities at the point $(x,\,0,\,z)$ due to two distributions of semi-infinite source lines joined at the crank. These velocities are :

$$\frac{v_x}{V_0}=\frac{1}{2}\left\{\frac{v_x'}{V_0}\cos\varphi-\frac{q(x)}{2V_0}\cos\varphi\,.f(\varphi)\right\}$$

and

$$\frac{v_y}{V_0}=-\frac{1}{4\pi V_0}\left(\sin\varphi\,.\,I_1+\frac{1}{\sin\varphi}I_2+\sin\varphi\,.\,I_3\right),$$

where

$$\frac{v_x'}{V_0}=\frac{1}{2\pi V_0}\int_0^1 q(x')\frac{dx'}{x-x'}$$

$$=\frac{1}{\pi}\int_0^1\frac{dz(x')}{dx'}\frac{dx'}{x-x'}$$

is the velocity component in the x-direction due to such a source distribution with $\varphi=0$ deg,

$$f(\varphi)=\frac{1}{\pi}\log\frac{1+\sin\varphi}{1-\sin\varphi}$$

and I_1, I_2 and I_3 are the three integrals which appear in section 2, with $q(x')$ replacing $\gamma(x')$.

I_1 and I_3 again have finite values at the point $(x, 0, 0)$, but I_2 is infinite in the plane $z = 0$. This kind of infinity occurs whenever source lines are cut off sharply, as at a wing tip. If we consider the two distributions of semi-infinite source lines, each distribution will induce an infinite velocity v_y at the crank in the plane $z = 0$. These two velocities will be in opposite directions, and their difference may be finite. Then the total velocity in the y-direction at a point $(x, 0, 0)$ will, in general, be finite and not zero. This means that there is a flow of source material across the crank. If the source strength is the same on each side of the crank (i.e., $q_i(x') = q_o(x')$) then the aerofoil section which is represented will be thinner on one side of the crank than on a similar sheared wing. Correspondingly the aerofoil section on the other side of the crank will be thicker than on the sheared wing. Therefore if the aerofoil section is to be kept constant everywhere the source distributions near the crank cannot be independent of y; they must vary with spanwise position to compensate for the distorting effect of the spanwise velocity v_y. Far from the crank, $q_i(x') = q_o(x')$ as before. The dependence of $q(x)$ on y is the stumbling-block to a solution on these lines. The calculation of the spanwise variation of $q(x)$ and the subsequent calculation of the velocities induced by the source distributions would be very long and complex and the procedure is quite unsuitable for a routine method.

The contribution to the v_y-velocity due to I_2 can be made finite by calculating it on the surface of the aerofoil instead of on the chord line (*i.e.*, in the plane $z = 0$), as was done for v_z in section 2.

Evaluating I_1, I_2 and I_3 as in Ref. 5, we get

$$\frac{v_y}{V_0} = -\tfrac{1}{2}\sin\varphi\,\frac{v_x'}{V_0} - \frac{q(x)}{4V_0}\cdot\frac{\tan\varphi + f(\varphi)}{\sin\varphi} + \frac{q(x)}{4V_0}f(\varphi)\sin\varphi\,.$$

If $\varphi = 0$ deg, then the first and third terms become zero, but the second term (evaluated on the aerofoil surface) becomes

$$-\frac{q(x)}{4V_0}\left(1 + \frac{2}{\pi}\right).$$

If we now combine the induced velocities due to the two semi-infinite source distributions, the velocity components at the crank are :

$$\frac{v_x}{V_0} = \frac{\cos\varphi_i + \cos\varphi_o}{2}\,\frac{v_x'}{V_0} + \frac{\cos\varphi_i\,.\,f(\varphi_i) \mp \cos\varphi_o\,.\,f(\varphi_o)}{2}\,\frac{q(x)}{2V_0} \qquad \ldots\ \ldots \qquad (15)$$

and

$$\frac{v_y}{V_0} = -\frac{\sin\varphi_i + \sin\varphi_o}{2}\,\frac{v_x'}{V_0}$$

$$+ \frac{q_i(x)}{4V_0}\left\{\frac{\tan\varphi_i + f(\varphi_i)}{\sin\varphi_i} - f(\varphi_i)\sin\varphi_i\right\}$$

$$- \frac{q_o(x)}{4V_0}\left\{\frac{\tan\varphi_o + f(\varphi_o)}{\sin\varphi_o} - f(\varphi_o)\sin\varphi_o\right\}. \qquad \ldots\ \ldots\ \ldots\ \ldots \qquad (16)$$

In general $v_y/V_0 \neq 0$ and the source distributions must vary spanwise, as shown above. The refinement of evaluating I_2 on the aerofoil surface has thus failed to simplify the calculation.

We therefore look for an approximate method for calculating the perturbation velocities which avoids the discontinuity and variation in $q(x)$ and the infinity in v_y. The first term in equations (15) and (16), *i.e.*, the term which is derived from sheared wing conditions, is retained. The effect of the crank—which will fade out to zero at some distance from the crank—is obtained by using the same conception as in section 2 for cranked vortex lines, *viz.*, the kink of a wing

April 1970
Jack has shown that = n 16 is wrong and that the argument from this point is fallacious.

swept at an angle φ^* and yawed at an angle $\frac{1}{2}(\varphi_i + \varphi_o)$ (Fig. 1b.) The source strength corresponding to such a wing is constant over the span and is given by .

$$q^*(X) = \frac{dz}{dX} = \frac{dz}{dx}\frac{dx}{dX}$$

$$= q(x)\frac{1}{\cos\varphi^*} \qquad \ldots\ldots\ldots\ldots\ldots\ldots\ldots\ldots \quad (17)$$

where $q(x)$ is the distribution of source strength in the x-direction at the sheared parts of the wing on either side of the crank : *i.e.*, it is based on the profile shape along wind. The X and Y-axes are drawn in Fig. 1b.

For such a distribution of source lines the perturbation velocity components in the X and Y directions are :

$$\frac{v_X}{V_0} = \cos\varphi^* \cdot \frac{v_X'}{V_0} - \cos\varphi^* \cdot f(\varphi^*)\frac{q^*(X)}{2V_0}$$

$$\frac{v_Y}{V_0} = 0 .$$

Then

$$\frac{v_x}{V_0} = \frac{v_X}{V_0}\cos\frac{\varphi_i + \varphi_o}{2}$$

$$\frac{v_y}{V_0} = -\frac{v_X}{V_0}\sin\frac{\varphi_i + \varphi_o}{2} .$$

From equation (17),

$$v_X' = v_x'\frac{1}{\cos\varphi^*} .$$

Therefore,

$$\frac{v_x}{V_0} = \cos\frac{\varphi_i + \varphi_o}{2}\cdot\frac{v_x'}{V_0} - \cos\frac{\varphi_i + \varphi_o}{2}\cdot f(\varphi^*)\frac{q(x)}{2V_0} .$$

The ' crank ' term in this expression is $-\cos\frac{1}{2}(\varphi_i + \varphi_o) \cdot f(\varphi^*)\, q(x)/2V_0$, which will be used in the final formula.

$$\frac{v_y}{V_0} = -\sin\frac{\varphi_i + \varphi_o}{2}\cdot\frac{v_x'}{V_0} + \sin\frac{\varphi_i + \varphi_o}{2}\cdot f(\varphi^*)\frac{q(x)}{2V_0}$$

which is neither infinite nor zero. The ' crank ' term in this expression is $\sin\frac{1}{2}(\varphi_i + \varphi_o) \cdot f(\varphi^*)\, q(x)/2V_0$, which will be used in the final formula.

The terms from the ' sheared wing ' equations are :

$$\frac{v_x}{V_0} = \frac{\cos\varphi_i + \cos\varphi_o}{2}\frac{v_x'}{V_0}$$

$$\frac{v_y}{V_0} = -\frac{\sin\varphi_i + \sin\varphi_o}{2}\frac{v_x'}{V_0} ,$$

i.e., the first terms in equations (15) and (16). Finally, combining ' crank ' and ' sheared wing ' terms, we obtain the equations :

$$\frac{v_x}{V_0} = \frac{\cos\varphi_i + \cos\varphi_o}{2} \cdot \frac{v_x'}{V_0} - \cos\frac{\varphi_i + \varphi_o}{2} \cdot f(\varphi^*)\,\frac{q(x)}{2V_0}$$

$$\frac{v_y}{V_0} = -\frac{\sin\varphi_i + \sin\varphi_o}{2} \cdot \frac{v_x'}{V_0} + \sin\frac{\varphi_i + \varphi_o}{2} \cdot f(\varphi^*)\,\frac{q(x)}{2V_0} \cdot$$

Let

$$\frac{v_x'}{V_0} = S_v^{(1)} \quad \text{and} \quad \frac{q(x)}{2V_0} = \frac{dz}{dx} \text{ (for a symmetrical section)}$$
$$= S_v^{(2)} .$$

$S_v^{(1)}$ and $S_v^{(2)}$ are related to the functions A_n and B_n of Ref. 11 (*see* section 4).

Then

$$\frac{v_x}{V_0} = \frac{\cos\varphi_i + \cos\varphi_0}{2} S_v^{(1)} - \cos\frac{\varphi_i + \varphi_0}{2} \cdot f(\varphi^*)\, S_v^{(2)} \qquad \ldots \quad \ldots \quad \ldots \qquad (18)$$

$$\frac{v_y}{V_0} = -\frac{\sin\varphi_i + \sin\varphi_0}{2} S_v^{(1)} + \sin\frac{\varphi_i + \varphi_0}{2} \cdot f(\varphi^*)\, S_v^{(2)} . \qquad \ldots \quad \ldots \quad \ldots \qquad (19)$$

Equations (18) and (19) give the linear perturbation velocities at the crank of a wing with symmetrical section at zero incidence. The chordwise pressure distribution follows from Bernoulli's equation

$$C_p(x) = 1 - \left(\frac{V}{V_0}\right)^2 = 1 - \left(\frac{V_X}{V_0}\right)^2 - \sin^2\varphi \quad \text{(equation (33) of Ref. 11).}$$

V_X here includes the factor

$$\frac{1}{1 + \left(\dfrac{S_v^{(2)}}{\cos\varphi}\right)^2},$$

a correction to allow for second-order effects which is significant near the leading edge. This correction, derived for infinite sheared wings in Ref. 11, is assumed to be true also for the present case at the crank. φ now becomes $\frac{1}{2}(\varphi_i + \varphi_o)$. Expressed in terms of x and y components of velocity, the above equation for the pressure coefficient becomes

$$C_p(x) = 1 - \frac{1}{1 + \left(S_v^{(2)}/\cos\dfrac{\varphi_i + \varphi_o}{2}\right)^2} \left\{ \left(1 + \frac{v_x}{V_0}\right)^2 + \frac{v_y^2}{V_0^2} + \sin^2\frac{\varphi_i + \varphi_0}{2} \cdot \frac{[S_v^{(2)}]^2}{\cos^2\dfrac{\varphi_i + \varphi_0}{2}} \right\}$$

where v_x and v_y are given by equations (18) and (19).

4. *The Chordwise Loading and Pressure Distribution at the Crank of an Infinite Thick Wing of Symmetrical Section at Incidence.*—By combining the results of sections 2 and 3, we can now obtain an expression for the chordwise pressure distribution at non-zero incidences. The velocities induced on the aerofoil surface by the vortex filaments are $+\frac{1}{2}\gamma(x)$ and $-\frac{1}{2}\gamma(x)$ perpendicular to the vorticity vector on the upper and lower surfaces respectively. Their components in the positive directions of x and y are then $\pm\frac{1}{2}\gamma(x)\cos\frac{1}{2}(\varphi_i + \varphi_o)$ and $\mp\frac{1}{2}\gamma(x)\sin\frac{1}{2}(\varphi_i + \varphi_o)$ respectively. The components of the free-steam velocity in the x and z directions are now $V_0\cos\alpha_{e0}$ and $-V_0\sin\alpha_{e0}$ respectively, where α_{e0} is the effective incidence.

Then

$$C_p(x) = 1 - \frac{1}{1 + \left(\frac{S_v^{(2)}}{\cos \frac{\varphi_i + \varphi_0}{2}} \right)^2} \times$$

$$\times \left[\left\{ \cos \alpha_{e0} \left(1 + \frac{\cos \varphi_i + \cos \varphi_0}{2} \cdot S_v^{(1)} - \cos \frac{\varphi_i + \varphi_0}{2} \cdot f(\varphi^*)\, S_v^{(2)} \right) \right.\right.$$

$$\left.\left. \pm \sin \alpha_{e0} \sin \pi n_0^* \cos \frac{\varphi_i + \varphi_0}{2} \left(\frac{1 - x}{x} \right)^{n_0^*} \left(1 + \frac{S_v^{(3)}}{\cos \frac{\varphi_i + \varphi_o}{2}} \right) \right\}^2 \right.$$

$$+ \left\{ \cos \alpha_{e0} \left(- \frac{\sin \varphi_i + \sin \varphi_0}{2} S_v^{(1)} + \sin \frac{\varphi_i + \varphi_0}{2} \cdot f(\varphi^*)\, S_v^{(2)} \right) \right.$$

$$\left. \mp \sin \alpha_{e0} \sin \pi n_0^* \sin \frac{\varphi_i + \varphi_0}{2} \left(\frac{1 - x}{x} \right)^{n_0^*} \left(1 + \frac{S_v^{(3)}}{\cos \frac{\varphi_i + \varphi_0}{2}} \right) \right\}^2$$

$$\left. + \cos^2 \alpha_{e0} \tan^2 \frac{\varphi_i + \varphi_0}{2} \cdot \left(S_v^{(2)} \right)^2 \right] . \quad .. \quad .. \quad .. \quad .. \quad .. \qquad (20)$$

$S_v^{(1)}$, $S_v^{(2)}$ and $S_v^{(3)}$ are functions of the aerofoil profile and are related to the functions a_n, A_n, B_n and G_n^* in Ref. 11 as follows :

$$S_v^{(1)} = - \frac{A_n}{a_n} \quad : \quad S_v^{(2)} = \frac{B_n}{a_n} \quad : \quad S_v^{(3)} = G_n^*$$

where a_n has the sign appropriate to the upper surface. v and n are corresponding suffixes indicating the chordwise pivotal points. $(1 + S_v^{(3)}/\cos \frac{1}{2}(\varphi_i + \varphi_o))$ is a factor to the velocity increments due to the vortices, to take account of the wing thickness.

n_0^* is given in section 2, and α_{e0} is the effective incidence, the suffix $_0$ in both cases indicating that we are dealing with a wing of infinite aspect ratio.

To a first-order approximation, the chordwise loading $\Delta C_p(x)$ can be obtained from thin-wing theory by using equation (14). A more exact answer which takes account of wing thickness can be obtained from equation (20) by subtracting $C_{p\ L.S.}$ from $C_{p\ U.S.}$:

$$\Delta C_p(x) = - \frac{4 \cos \alpha_{e0} \sin \alpha_{e0} \sin \pi n_0^* \left(\frac{1 - x}{x} \right)^{n_0^*} \left(1 + \frac{S_v^{(3)}}{\cos \frac{\varphi_i + \varphi_o}{2}} \right)}{1 + \left(\frac{S_v^{(2)}}{\cos \frac{\varphi_i + \varphi_0}{2}} \right)^2} \times$$

$$\times \left[\begin{array}{l} \cos \frac{\varphi_i + \varphi_o}{2} \left\{ 1 + \frac{\cos \varphi_i + \cos \varphi_o}{2} S_v^{(1)} - \cos \frac{\varphi_i + \varphi_o}{2} \cdot f(\varphi^*)\, S_v^{(2)} \right\} \\ - \sin \frac{\varphi_i + \varphi_o}{2} \left\{ - \frac{\sin \varphi_i + \sin \varphi_o}{2} S_v^{(1)} + \sin \frac{\varphi_i + \varphi_o}{2} \cdot f(\varphi^*)\, S_v^{(2)} \right\} \end{array} \right] . \qquad (21)$$

5. *The Loading of a Finite Cranked Wing.*—Sections 2, 3 and 4 have dealt with conditions at the crank of a wing stretching to infinity in both directions from the crank. The crank effect is thus isolated. On a real wing, the pressure distribution and loading at the crank are affected by the fact that the aspect ratio is finite and they may also be influenced by the centre and tip effects if the aspect ratio is small enough for these to overlap the crank.

5.1. *Wings of Symmetrical Section.*—The chordwise loading at any spanwise position on a wing of symmetrical section is characterised by the parameter n, which depends not only on sweep and spanwise position but also on aspect ratio. For an infinite cranked wing it has already been seen in section 2 that

$$n = n_0{}^* = \tfrac{1}{2}\left(1 - \lambda_{\text{cr.}}\frac{\varphi^*}{\pi/2}\right)$$

$$= 1 - \frac{1 + \lambda_{\text{cr.}}\dfrac{\varphi^*}{\pi/2}}{2}.$$

For a wing of very large aspect ratio such that the assumptions of section 2 still hold,

$$n = n_0{}' = \tfrac{1}{2}\left(1 - \lambda_{\text{cr.}}\frac{\varphi^*}{\pi/2} - \lambda_{\text{c}}\frac{\varphi_{\text{c}}}{\pi/2} - \lambda_{\text{T}}\frac{\varphi_{\text{T}}}{\pi/2}\right)$$

$$= 1 - \frac{1 + \lambda_{\text{cr.}}\dfrac{\varphi^*}{\pi/2} + \lambda_{\text{c}}\dfrac{\varphi_{\text{c}}}{\pi/2} + \lambda_{\text{T}}\dfrac{\varphi_{\text{T}}}{\pi/2}}{2} \quad .. \quad .. \quad .. \quad .. \quad (22)$$

at any spanwise position.

φ_{c}, φ_{T} are the sweep angles of the mid-chord lines of the wing panels adjacent to the centre-section and tip-section respectively.

λ_{c}, λ_{T}, are functions of the spanwise distance of the section from the centre and tip respectively. $\lambda_{\text{c}} \geqslant 0$, $\lambda_{\text{T}} \leqslant 0$ and $\lambda_{\text{cr.}} \geqslant 0$. The magnitudes of λ_{c} and λ_{T} may be obtained from Fig. 1 of Ref. 5, Fig. 1 of Ref. 7 or Fig. 23 of Ref. 6, or from equation (9), y being measured, in terms of the local chord, from the centre and tip respectively.

If there is more than one crank, the term $\lambda_{\text{cr.}}\,\varphi^*/\frac{1}{2}\pi$ becomes $\Sigma\lambda_{\text{cr.}}\,\varphi^*/\frac{1}{2}\pi$.

If now we consider a practical wing of finite aspect ratio and symmetrical section, it is shown in Ref. 6 that a factor

$$\frac{1}{\left\{1 + \left(\dfrac{a_0 \cos\varphi_m}{\pi A}\right)^2\right\}^{\frac{1}{4(1 + |\varphi_m|/\frac{1}{2}\pi)}}}$$

must be applied to the second term in the above equation, where

A is the aspect ratio of the whole wing,

φ_m is a mean sweep angle for the whole wing, obtained as the sweep of the line joining the mid-chord points of the centre and tip sections.

Therefore the general formula for n at any section of a finite cranked wing (single crank) is

$$n = 1 - \frac{1 + \lambda_{\text{cr.}}\dfrac{\varphi^*}{\pi/2} + \lambda_{\text{c}}\dfrac{\varphi_c}{\pi/2} + \lambda_{\text{T}}\dfrac{\varphi_{\text{T}}}{\pi/2}}{2\left\{1 + \left(\dfrac{a_0 \cos\varphi_m}{\pi A}\right)^2\right\}^{\frac{1}{4(1 + |\varphi_m|/\frac{1}{2}\pi)}}}, \quad .. \quad .. \quad .. \quad .. \quad (23)$$

and this value of n has to be inserted in the expression for the chordwise vortex distribution at that section.

Wings of finite aspect ratio may be tapered and in such cases, if the aspect ratio is large, the sweep angles taken, *viz.*, φ_c, φ_T, φ_i, φ_o, etc., are those of the mid-chord lines of the appropriate wing panels. As the aspect ratio gets smaller, however, there is a tendency for the sweep effect to become less and this may be allowed for by defining a new angle of sweep, namely the 'effective sweep,' φ_e (*see* Ref. 6). Since the different wing panels have different mid-chord sweeps, their effective sweeps will also be different and must be worked out separately. φ_e is thus different from φ_m, which represents an overall mean sweep of the whole wing. For any wing panel, a suitable approximation to φ_e is the sweep of the line joining the aerodynamic centres at the inboard and outboard edges of the panel. These aerodynamic centres may be calculated using the mid-chord sweep angles and the relation $x_{a.c.} = \frac{1}{2}(1 - n)$. φ_m is then also defined in terms of the aerodynamic centres, namely the sweep of the line joining the aerodynamic centres at root and tip.

For wings without cranks, φ_e is the same over the whole wing (and equal to φ_m), and can be approximated by :

$$\varphi_e = \frac{\varphi}{\left\{1 + \left(\frac{a_0 \cos \varphi_m}{\pi A}\right)^2\right\}^{1/4}} .$$

For cranked wings no such simple relation can be given since the aerodynamic centres on any panel may depend on the wing geometry outside the panel. φ_e is used instead of the mid-chord sweep in all loading calculations for wings of fairly small aspect ratio.

As a numerical example, an uncranked, constant-chord wing of 45-deg sweep would have the following effective sweeps :

$$\begin{aligned} A = 3 &, \varphi_e = 42{\cdot}6 \text{ deg} \\ 2 &, \varphi_e = 40{\cdot}5 \text{ deg} \\ 1 &, \varphi_e = 34{\cdot}2 \text{ deg} . \end{aligned}$$

The difference between effective and mid-chord sweeps on a cranked wing will be greatest on wings of M and W plan-form. In the calculations for such wings described in section 7, mid-chord sweep angles have been used. If φ_e had been used, the sweep of each wing panel would have been reduced by 4 to 6 deg.

Now that n is known from equation (23) we can go on to find the chordwise loading $\Delta C_p(x)$. As in Ref. 6, it is assumed that at each spanwise position

$$\Delta C_p(x) = -\frac{\sin \pi n}{\pi n} C_L \left(\frac{1 - x}{x}\right)^n \qquad (24)$$

where C_L is the local lift coefficient. This relation can be deduced, for the neighbourhood of the crank, from the formulae of section 2. The relation between $\gamma(x)$ and $\Delta C_p(x)$ now has to take account of the effect of the centre, crank and tip on the sweep of the vortex lines. As before,

$$\Delta C_p(x) = -2\frac{\gamma(x)}{V_0} \cos \varphi_V , \qquad (10)$$

and near an isolated centre or tip, a reasonable approximation is :

$$\cos \varphi_V = \frac{\cos \varphi}{\sin \pi n_0} ,$$

where

$$n_0 = 1 - \frac{1 + \lambda_c \frac{\varphi_c}{\pi/2} + \lambda_T \frac{\varphi_T}{\pi/2}}{2}$$

(*see* Ref. 7). When a crank is also present, we apply the interpolation factor used in section 2 so that

$$\Delta C_p(x) = -2\frac{\gamma(x)}{V_0} \frac{\cos \varphi}{\sin \pi n_0} \frac{\cos\left[\lambda_{cr.} \frac{\varphi_i + \varphi_o}{2}\right]}{\cos\left[\lambda_{cr.} \varphi\right]} . \qquad (25)$$

φ is the mid-chord sweep or effective sweep of the particular wing panel being considered. At an isolated centre or tip, $\lambda_{cr.} = 0$ and we return to equation (10) : at an isolated crank, $\lambda_{cr.} = 1$ and $\sin \pi n_0 = \sin \frac{1}{2}\pi = 1$ and we return to equation (13). If there is more than one crank between the centre and the tip, equation (25) becomes

$$\Delta C_p(x) = -2\frac{\gamma(x)}{V_0}\frac{\cos\varphi}{\sin \pi n_0} \Pi \frac{\cos\left[\lambda_{cr.}\dfrac{\varphi_i + \varphi_o}{2}\right]}{\cos\left[\lambda_{cr.}\varphi\right]},$$

where Π is the product of the terms $\cos\left[\lambda_{cr.}\frac{1}{2}(\varphi_i + \varphi_o)\right]/\cos\left[\lambda_{cr.}\varphi\right]$ from all the cranks.

Combining equations (24) and (25), for a single crank between centre and tip,

$$\gamma(x) = \frac{C_L V_0}{2}\frac{\sin \pi n}{\pi n}\frac{\sin \pi n_0}{\cos\varphi}\frac{\cos\left[\lambda_{cr.}\varphi\right]}{\cos\left[\lambda_{cr.}\dfrac{\varphi_i + \varphi_o}{2}\right]}\left(\frac{1-x}{x}\right)^n \quad \ldots \quad \ldots \quad \ldots \quad (26)$$

Thus equations (24), (25) and (26) give the relationship between $\gamma(x)$, $\Delta C_p(x)$ and C_L on a single-cranked wing. C_L still has to be found from the spanwise loading, and before that can be calculated the effect of finite aspect ratio on the sectional lift slope, a, must be considered.

When the aspect ratio is so small that fundamental assumptions based on the flow past a cranked wing of infinite span are no longer valid (*i.e.*, below about 6), then the effective incidence α_e is taken to be

$$\alpha_e = \int_0^1 \alpha_{e0}(x)\,dx \qquad (x \text{ is dimensionless with the chord}),$$

i.e., the mean value over the chord of $\alpha_{e0}(x)$, which is the effective incidence of a wing having the same chordwise vortex distribution as the finite wing, but extending to infinity on each side of the section considered. We can thus follow a similar development to that of section 2 and use the results derived there. The downwash equations (4) for a kink section and (5) for a crank section can be generalised for any section by replacing the factors to $\gamma(x)$, *viz.*, $\tan\varphi$ $(= 1/\tan \pi n_0)$ and $\tan\varphi^*$ $(= 1/\tan \pi n_0^*)$, by $1/\tan \pi n_0'$, where n_0' is given by equation (22). This gives the following downwash equation for the present wing.

$$\alpha_{e0}(x) = \frac{v_z}{V_0} = \frac{1}{2\pi V_0}\left\{\int_0^1 \gamma(x')\frac{dx'}{x - x'} + \frac{\pi}{\tan \pi n_0'}\gamma(x)\right\} \quad \ldots \quad \ldots \quad \ldots \quad (27)$$

Substituting for $\gamma(x)$ from equation (26),

$$\alpha_{e0}(x) = \frac{C_L}{4\pi}\frac{\sin \pi n}{\pi n}\frac{\sin \pi n_0}{\cos\varphi}\frac{\cos\left[\lambda_{cr.}\varphi\right]}{\cos\left[\lambda_{cr.}\dfrac{\varphi_i + \varphi_o}{2}\right]}\left\{\frac{\pi}{\sin \pi n} - \left(\frac{\pi}{\tan \pi n} - \frac{\pi}{\tan \pi n_0'}\right)\left(\frac{1-x}{x}\right)^n\right\}$$

$$\alpha_e = \int_0^1 \alpha_{e0}(x)\,dx$$

$$= \frac{C_L}{4\pi}\frac{\sin \pi n}{\pi n}\frac{\sin \pi n_0}{\cos\varphi}\cdot\frac{\cos\left[\lambda_{cr.}\varphi\right]}{\cos\left[\lambda_{cr.}\dfrac{\varphi_i + \varphi_o}{2}\right]}\left\{\frac{\pi}{\sin \pi n} - (\pi\cot \pi n - \pi\cot \pi n_0')\frac{\pi n}{\sin \pi n}\right\}$$

$$= \frac{C_L}{2n\,a_0}\frac{\sin \pi n_0}{\cos\varphi}\frac{\cos\left[\lambda_{cr.}\varphi\right]}{\cos\left[\lambda_{cr.}\dfrac{\varphi_i + \varphi_o}{2}\right]}\{1 - \pi n\,(\cot \pi n - \pi n_0')\}.$$

on putting $2\pi = a_0$. Therefore the sectional lift slope at any spanwise position on a thin cranked wing of finite aspect ratio is

$$a = \frac{C_L}{\alpha_e} = a_0 \frac{2n}{1 - \pi n(\cot \pi n - \cot \pi n_0')} \frac{\cos \varphi}{\sin \pi n_0} \frac{\cos\left[\lambda_{cr.} \frac{\varphi_i + \varphi_0}{2}\right]}{\cos\left[\lambda_{cr.} \varphi\right]} \quad \ldots \quad (28)$$

a_0 is the two-dimensional lift slope of the aerofoil section and is 2π for a thin wing. However thickness and viscosity effects can be allowed for by taking $a_0 = k.2\pi\{1 + (0{\cdot}8\, t/c)/\cos\varphi\}$, where k is a factor to take account of the reduction in lift due to the boundary layer[12] : $k \sim 0{\cdot}9$. $\{1 + (0{\cdot}8\, t/c)/\cos\varphi\}$ is a factor to allow for the thickness of the wing, t/c being the thickness/chord ratio in the wind direction. At the crank itself, a_0 changes discontinuously from its value with $\varphi = \varphi_i$ to its value with $\varphi = \varphi_o$. Normally the two values will not differ by very much and the arithmetic mean may be used at the crank. It will be noticed that in the limits when the crank becomes a sheared wing section (i.e., $\varphi_i = \varphi_o$) or a kink section ($\varphi_i = -\varphi_o$), the lift slope equation becomes the same as those given in Ref. 6 for the two cases. In the former, $\frac{1}{2}(\varphi_i + \varphi_o) = \varphi$, $\varphi^* = 0$, $n_0 = n_0' = \frac{1}{2}$, and

$$a = a_0 \frac{2n \cos \varphi}{1 - \pi n \cot \pi n} \quad \text{(equation (78) of Ref. 6).}$$

In the latter case, $\frac{\varphi_i + \varphi_o}{2} = 0$, $\varphi^* = \varphi$, $n_0 = \frac{1}{2}$ and

$$a = a_0 \frac{2n}{1 - \pi n(\cot \pi n - \cot \pi n_0')}.$$

We can now go on to calculate the spanwise loading using equation (16) of Ref. 6 :

$$\gamma_\nu \left(b_{\nu\nu} + \frac{2b}{\omega a_\nu c_\nu} \right) = \frac{\alpha_\nu}{\omega} + \sum_{n=1}^{m}{}' b_{\nu n} \cdot \gamma_n \quad \ldots \quad (29)$$

(notation as in Ref. 6).

In this equation a_ν is found from equation (28) above, and the downwash factor ω is found from equation (89) of Ref. 6 in which φ is the angle φ_m of the cranked wing, *i.e.*,

$$\omega = 2 - \frac{1}{\left\{1 + \left(\frac{a_0 \cos \varphi_m}{\pi A}\right)^2\right\}^{\frac{1}{4(1 + |\varphi_m|/\frac{1}{2}\pi)}}} \quad \ldots \quad (30)$$

Owing to the presence of the crank and the more rapid spanwise variations of C_L which it introduces, it may be advisable to calculate a 31-point solution instead of the more usual 15-point solution. The spanwise positions of the pivotal points and the Multhopp coefficients for $m = 31$ are given in Ref. 4.

The chordwise loading at any section is obtained from equation (24). n is given by equation (23) and $C_L = a\alpha_e$. α_e is the difference between the geometric incidence of the section and the induced incidence from the trailing vortices, which follows from the spanwise loading calculation.

The chordwise pressure distribution is given by a similar equation to (20). However, the incidence term must be modified to take account of the finite aspect ratio and centre and tip effects, since $\gamma(x)$ is given by equation (26) instead of equation (7) as for an infinite wing. Then the chordwise pressure distribution at the crank becomes

$$C_p(x) = 1 - \frac{1}{1 + \left(\dfrac{S_v^{(2)}}{\cos\dfrac{\varphi_i + \varphi_o}{2}}\right)^2} \times$$

$$\times \left[\left\{ \cos\alpha_e \left[1 + \frac{\cos\varphi_i + \cos\varphi_o}{2} S_v^{(1)} - \cos\frac{\varphi_i + \varphi_o}{2} f(\varphi^*)\, S_v^{(2)} \right] \right.\right.$$

$$\left.\left. \pm \frac{C_L}{4} \cdot \frac{\sin\pi n}{\pi n} \left(\frac{1-x}{x}\right)^n \left(1 + \frac{S_v^{(3)}}{\cos\dfrac{\varphi_i + \varphi_o}{2}}\right) \right\}^2 \right.$$

$$+ \left\{ \cos\alpha_e \left[-\frac{\sin\varphi_i + \sin\varphi_o}{2} S_v^{(1)} + \sin\frac{\varphi_i + \varphi_o}{2} f(\varphi^*)\, S_v^{(2)} \right] \right.$$

$$\left. \mp \frac{C_L}{4} \frac{\sin\pi n}{\pi n} \frac{\sin\varphi_V}{\cos\varphi_V} \left(\frac{1-x}{x}\right)^n \left(1 + \frac{S_v^{(3)}}{\cos\dfrac{\varphi_i + \varphi_o}{2}}\right) \right\}^2$$

$$\left. + \cos^2\alpha_e \tan^2\frac{\varphi_i + \varphi_o}{2} [S_v^{(2)}]^2 \right]. \qquad (31)$$

5.2. *Cambered Wings.*—The method described in Ref. 7 for calculating the loadings and pressure distribution over swept wings with cambered sections may be easily applied to cranked wings with cambered sections. This method is strictly applicable only to wings for which low aspect-ratio corrections can be neglected (i.e., $A \geqslant$ about 3). The family of camber lines of Ref. 7 and their aerodynamic characteristics were derived from the same type of downwash equation as equations (4), (5) and (27) of the present report, and thus the results may be applied directly to cranked wings.

Consider first a given cranked wing with a cambered section. The spanwise loading is calculated as explained in section 4.1 of Ref. 7. In the present case however, the lift slope, a, is obtained from equation (28), and ω from equation (30). The only remaining parameter to be inserted in the spanwise loading equation (equation (58) of Ref. 7 is equivalent to equation (29) of this report when the ω term has been included) is the equivalent incidence of the camber line, $\Delta\alpha$, at the various pivotal points. This can be read directly from Figs. 6 and 7 of Ref. 7 as before : but in the case of a cranked wing the quantity $\lambda\varphi$ against which $\Delta\alpha/f$ is plotted becomes $\Sigma\lambda\varphi = \lambda_c\varphi_c + \lambda_T\varphi_T + \lambda_{cr.}\varphi^*$. This is necessary because, on a cranked wing, centre, crank and tip effects may overlap even at fairly high aspect ratios. The chordwise loading at any spanwise position is calculated from equation (32) and section 4.1.3. of Ref. 7. The chordwise pressure distribution at the crank may be obtained from equation (31) of the present report with the camber effect added :

$$C_p(x) = 1 - \frac{1}{1 + \left(\dfrac{S_v^{(2)} \pm S_v^{(4)}}{\cos\dfrac{\varphi_i + \varphi_o}{2}}\right)^2} \times$$

$$\times \left[\left\{ \cos\alpha_{e0} \left[1 + \frac{\cos\varphi_i + \cos\varphi_o}{2} S_v^{(1)} - \cos\frac{\varphi_i + \varphi_o}{2} . f(\varphi^*)\, S_v^{(2)} \right] \right.\right.$$

$$\left.\left. \pm \frac{\cos\varphi_V}{2V_0} \left[\gamma(x)_a \left(1 + \frac{S_v^{(3)}}{\cos\dfrac{\varphi_i + \varphi_o}{2}} \right) + \gamma(x)_f \right] \right\}^2 \right.$$

$$+ \left\{ \cos\alpha_{e0} \left[- \frac{\sin\varphi_i + \sin\varphi_0}{2} S_v^{(1)} + \sin\frac{\varphi_i + \varphi_0}{2} f(\varphi^*)\, S_v^{(2)} \right] \right.$$

$$\left. \mp \frac{\sin\varphi_V}{2V_0} \left[\gamma(x)_a \left(1 + \frac{S_v^{(3)}}{\cos\dfrac{\varphi_i + \varphi_o}{2}} \right) + \gamma(x)_f \right] \right\}^2$$

$$\left. + \cos^2\alpha_{e0} \tan^2\frac{\varphi_i + \varphi_o}{2} (S_v^{(2)} \pm S_v^{(4)})^2 \right] . \qquad .. \qquad .. \qquad .. \qquad (32)$$

α_{e0} is used because fairly high aspect ratio is assumed.

$\gamma(x)_a$, the vortex distribution due to incidence is given by equation (7) or by equation (26)† with $n = n_0{}^*$, and $\gamma(x)_f$, the vortex distribution due to camber, is given by :

$$\gamma(x)_f = 2V_0 \,.\, 4{\cdot}53 \,.\, C(m) \,.\, f\left(\frac{1-x}{x}\right)^m \times$$

$$\times \left[\frac{1}{\pi m(\cot\pi m - \cot\pi n)} - \frac{\sin\pi n}{\sin\pi m} \left(\frac{1}{\pi m(\cot\pi m - \cot\pi n)} - 1 \right) \left(\frac{1-x}{x} \right)^{n-m} \right] \qquad (33)$$

from equation (28) of Ref. 7.

$S_v^{(4)}$ is the slope of the camber-line and in the notation of Ref. 11, $S_v^{(4)} = (D_n/a_n)_{\text{U.S.}}$.

It has already been pointed out in section 2 that, physically, a crank has the same sort of effect on the pressures and loadings on a wing as has the kink of a swept-back or swept-forward wing. If, as is usual, the sweep decreases towards the tips, the effect will be similar to a swept-forward kink. There will be high suction peaks near the nose of the crank section and the chordwise loading will also be concentrated near the nose. If these peaks are to be eliminated without loss of lift, camber and twist must be applied to the basic aerofoil section in the neighbourhood of the crank. The camber and twist should be properly matched to each other to give the required chordwise loading, and to do this the procedure of section 4.2 of Ref. 7 can be followed. For instance, on a thin high aspect ratio wing with symmetrical section and one crank, the chordwise loading at the crank is

$$\Delta C_p(x) = -\,4[\alpha_{e0}]_{\text{cr.}} \sin\pi n_0{}^* \cos\frac{\varphi_i + \varphi_o}{2} \left(\frac{1-x}{x} \right)^{n_0{}^*}$$

and

$$\gamma(x) = 2V_0\,[\alpha_{e0}]_{\text{cr.}} \sin\pi n_0{}^* \,.\, \left(\frac{1-x}{x} \right)^{n_0{}^*} .$$

† It should be noted that C_L in equation (26) is the local lift coefficient due to incidence only.

Suppose we want to incorporate camber and twist so that the chordwise loading at the crank is like that on a sheared wing of symmetrical section and sweep equal to $\frac{1}{2}(\varphi_i + \varphi_o)$ at an effective incidence $[\alpha_{e0}]_s$. This would eliminate the excessive suction peaks at the crank and produce a smooth spanwise pressure distribution. The required loading is

$$\Delta C_p(x) = -4\,[\alpha_{e0}]_s \cos\frac{\varphi_i + \varphi_o}{2} \cdot \left(\frac{1-x}{x}\right)^{1/2}$$

and

$$\gamma(x) = 2V_0\,[\alpha_{e0}]_s \left(\frac{1-x}{x}\right)^{1/2}.$$

The suffices $_{cr.}$ and $_s$ refer to the crank and sheared wing conditions respectively.

Following the method of section 4.2.2 of Ref. 7, the required camber line at the crank is given by :

$$[z(x)]_{cr.} = \frac{\cot \pi n_0^*}{2}\,[\alpha_{e0}]_s \left[\frac{\pi}{2}(1-2x) - \sin^{-1}(1-2x) + \sqrt{\{1-(1-2x)^2\}}\right]$$

and the required effective incidence at the crank by :

$$[\alpha_{e0}]_{cr.} = \left(1 + \frac{\pi}{2}\cot \pi n_0^*\right)[\alpha_{e0}]_s .$$

It should be noted that z is measured positive downwards.

If the basic section itself has a camber the more general results of section 4.2.2 of Ref. 7 may be similarly applied.

Hitherto in this section it has been assumed that the wing has an aspect ratio of about 3 or greater. The effect of low aspect ratio on the camber characteristics derived in Ref. 7 is not yet known, but an estimate of the loading and pressure distribution of a cambered cranked wing with $A < 3$ could be made on the basis of the high aspect ratio characteristics. That is, equation (32) would still be used for the chordwise pressure distribution with α_{e0} replaced by α_e from section 5.1, n given by equation (23) and $\gamma(x)_a$ by equation (26).

6. *Comparison Between Experiment and Calculation.*—6.1. *Constant-chord, Cranked Wing, $A = 5$ (Wing I).*—A test was made in the No. 2, 11½-ft × 8½-ft Wind Tunnel at the Royal Aircraft Establishment in September, 1951, on a constant-chord cranked wing of aspect ratio 5. The crank was at a spanwise position $\eta = y.c/\frac{1}{2}b = 0{\cdot}5$ (i.e., $y = 1{\cdot}25$), the sweep of the inboard panel being 45 deg and that of the outboard panel 0 deg. A sketch of the plan-form is given in Fig. 2b. The wing was modified from Wing C of Ref. 13 and thus near the centre section it had camber and twist applied to the basic symmetrical section, RAE 101, $t/c = 0{\cdot}12$. This camber and twist modification decreased rapidly away from the centre and had become zero by $y = 1{\cdot}00$, *i.e.*, at $0{\cdot}25c$ from the crank section. Thus the flow conditions at the crank were not likely to be affected.

The test consisted of static-pressure measurements by means of flush holes on both surfaces of the wing at the crank section, at incidences from $-2{\cdot}2$ deg to $+11{\cdot}1$ deg. These pressure distributions were integrated to give the local normal force coefficients at the crank.

The chordwise pressure distribution at the crank and the chordwise and spanwise loadings have been calculated for Wing I, using the formulae developed in section 5. The experimental data are compared with the calculations in Figs. 3 to 11. Fig. 3 shows the experimental and calculated chordwise pressure distribution at zero incidence. The agreement is good enough to justify the suppositions made in deriving the expressions for the velocity increments due to

wing thickness in section 3. Pressure distributions at incidences up to $11 \cdot 1$ deg are shown in Fig. 4. The agreement between experiment and calculation is good at $\alpha = 2 \cdot 2$ deg, but becomes less good as the incidence increases. Over most of the section the pressure becomes greater than calculated and over the last 5 to 10 per cent of the chord it becomes less than calculated. This is consistent with the effect of viscosity. The boundary layer effectively reduces the incidence and on the greater part of the section the upper surface pressures are correspondingly increased. At the rear of the section the pressure is no longer constant through the thick boundary layer and is less than the potential-flow value. This is noticeable even at zero incidence (Fig. 3) ; it is of the same order but somewhat greater than one would expect on a two-dimensional section because of the steeper adverse pressure gradient which thickens the boundary layer. Moreover, at the crank section the spanwise boundary layer flow characteristic of swept wings may combine with the chordwise flow over the unswept panel to thicken the boundary layer.

Fig. 4 shows that the flow separated at the rear of the section at the higher incidences. This separation is just starting at $\alpha = 8 \cdot 8$ deg and extends over the rear 30 per cent of the chord at $11 \cdot 1$ deg.

The chordwise loading at the crank (i.e., $C_{p\,\text{U.S.}} - C_{p\,\text{L.S.}} = \Delta C_p$) at $\alpha = 2 \cdot 2$ deg is plotted in Fig. 5 and compared with calculations by thin-wing theory and the more complete thick-wing method. It can be seen that both methods give reasonable agreement, with the thick-wing distribution rather more accurate. The effective incidence used in the calculations included the factor $k = 0 \cdot 92$ to take account of the overall viscosity effects on a corresponding two-dimensional wing at $C_L = 0$[12, 14]. Even so, some additional viscosity effect is still noticeable near the rear of the section, which means that k must be less than $0 \cdot 92$ at the crank.

Fig. 6 shows the chordwise loadings at the crank and at a 45-deg sheared wing, plotted so that the effects of viscosity may be clearly seen. The experimental results are extrapolated to $\alpha = 0$ deg, thus eliminating those boundary-layer effects which vary non-linearly with lift. The factor $k = 0 \cdot 92$ was used in both calculations and the values of C_L/α obtained by chordwise integration show that it gives good agreement in the case of the sheared wing, but that it underestimates slightly the viscosity effect at the crank. It can be seen from the figure that the discrepancy occurs at the rear of the section where the boundary layer must be thicker than on the sheared wing. A value of $k = 0 \cdot 90$ is appropriate to the crank section.

Fig. 7 shows the chordwise loadings at $\alpha = 8 \cdot 8$ deg and $\alpha = 11 \cdot 1$ deg. Here the discrepancies between calculated and experimental values are much greater, even though the factor $k = 0 \cdot 92$ is again included in the calculation. This indicates the effect on k of the thickening of the boundary layer with lift, but an accurate estimate of k is not possible since an experimental spanwise loading is not available. A rough estimate, however, shows that the boundary layer thickens more rapidly with lift than on the two-dimensional wing of Ref. 12 and at approximately the same rate as on the sheared part of a 45-deg swept wing[15]. There is a slight increase in lift at the rear of the section at $\alpha = 11 \cdot 1$ deg due to the separation, which can be clearly seen in Fig. 7. The separation is just starting at $\alpha = 8 \cdot 8$ deg.

The high loading near the nose of the crank section is well shown in Fig. 8, in which experimental values of $\Delta C_p/\alpha$ (extrapolated to $\alpha = 0$ deg) are plotted for the crank section and for the centre-section and sheared part of a 45-deg constant-chord swept wing of aspect ratio 5 with 12 per cent RAE 101 section (Wing A of Ref. 13). The calculated distributions for these sections are also shown. The calculated peak at the crank section is not plotted but is approximately equal to 60, *i.e.*, nearly four times as great as the peak on the 45-deg sheared wing. Admittedly the difference in sweep between inboard and outboard panels on the present model, *viz.*, 45 deg, is considerably greater than has been usual up to the present, but it is not excessive compared with the M, W, and Λ plan-forms being investigated for structural reasons[1,2,16]. The existence of such large local suctions and forces must therefore be recognised when these plan-forms are being considered.

The calculated spanwise loading of Wing I is plotted in Fig. 9, along with the calculated loadings for the corresponding unswept and fully-swept-back (45-deg) wings. The spanwise variation of lift slope is plotted in Fig. 10 and the local induced drag in Fig. 11.

Fig. 9 shows that, as one would expect, the local lift coefficient changes gradually from roughly the swept-wing value at the centre towards the unswept-wing value near the tip. The only experimental point is the C_L at the crank section obtained by integrating the chordwise pressure distributions. (As $\alpha \to 0$, $C_N \to C_L$). As with the chordwise loading, the spanwise loading calculation includes the two-dimensional viscosity factor, $k = 0{\cdot}92$, to the local lift slopes, and the discrepancy between the experimental and calculated C_L at the crank is due to the boundary layer being thicker than on a two-dimensional wing. As seen above, $k = 0{\cdot}90$ at the crank.

Since decrease of sweep near the tip is often considered as a possible means of alleviating tip stalling, Fig. 9 poses the question whether any real improvement is likely to come about by this means. It has already been shown in Ref. 14 that leading-edge separation may take place first near mid-semi-span on a swept wing. On the present wing, the local lift coefficient is higher there than elsewhere and the chordwise pressure distribution is very 'peaky,' so that separation is likely to occur first at that section. Moreoever, the breakdown of flow may still spread outboard rapidly as in Ref. 14, since the C_L values outboard of the crank are higher than on the fully swept wing, and may offset the flatter pressure distribution on the unswept panel. The data from Wing I, however, probably present too pessimistic a view of the problem owing to the constant chord near the tip.

If camber and twist were applied to the crank of Wing I to restore a sheared-wing chordwise loading, as described in section 5.2, the amounts of camber and twist required would be

$$z_{\text{cr.}} = -\,0{\cdot}2504\,[\alpha_e]_s\left\{\frac{\pi}{2}(1-2x) - \sin^{-1}(1-2x) + \sqrt{[1-(1-2x)^2]}\right\}$$

and

$$[\alpha_e]_{\text{cr.}} = 0{\cdot}214\,[\alpha_e]_s\,.$$

The camber is positive in the usual sense, since z is measured positive downwards. If $[\alpha_e]_s = 2$ deg, the camber required ~ 1 per cent.

Fig. 11 shows the spanwise variation of local induced drag. The high value at the crank may be offset in the low incidence range by the reduction in the drag induced by the bound vortices, owing to the 'peaky' pressure distribution. In the present example there is in fact a thrust at the crank instead of a form drag. This thrust is the same as that found at the tip of a fully-swept wing, and counterbalances the form drag at the centre-section, since there can be no net drag or thrust force in potential flow.

6.2. *Double-cranked Wing (Ref. 17).*—The spanwise loading has been calculated for the wing of Ref. 17 which has two cranks between centre and tip and an aspect ratio of 4. The change of angle of mid-chord sweep in each case is of the order of 10 deg so that the crank effects are much more gentle than in the case of Wing I. The calculated loading is compared with the experimental local lift coefficients in Fig. 12, the agreement being quite good. Owing to the small changes of sweep however, the spanwise loading does not differ much from that of a wing of constant sweep, as can be seen from the calculated loading for a wing swept at an angle of 19·6 deg, which is the sweep of the middle panel of the cranked wing. A similar calculation using the mean sweep, $\varphi_m = 21{\cdot}3$ deg was not significantly different. Even though the spanwise loadings are nearly the same, the chordwise loadings near the cranks will be appreciably different from those calculated on the basis of a uniformly swept wing. They have higher suction peaks further forward, and one can expect viscosity effects to be rather more noticeable.

7. *Comparison with Other Calculation Methods.*—Two recent American reports[1,2] have dealt with the calculation of the spanwise loadings of wings having M, W and Λ plan-forms. Both of these methods replace the wing by a series of horseshoe vortices, each of which is centred on the quarter-chord line. The downwash due to these vortices is calculated on the intersection of the three-quarter-chord line with their axes of symmetry. Three of the wing plan-forms considered in Ref. 1 have been calculated by the method of the present report and the results are given in Figs. 13 and 14. Fig. 13 shows the most extreme cases of M and W plan-form likely to occur, and Fig. 14 shows a wing with similar sweep characteristics to Wing I (section 6.1) but with the crank at $\eta = 0{\cdot}3$ instead of $0{\cdot}5$, and a taper ratio of $0{\cdot}5$ instead of $1{\cdot}0$.

It is clear that as far as the results of these spanwise loading calculations are concerned there is little to choose between the present method and that of Ref. 1. With regard to the aerodynamic centre, the simple approximations of Ref. 1 seem to be inadequate for predicting the spanwise variations, and discrepancies up to $0{\cdot}05c$ are apparent between the two methods.

Apart from specific examples, however, the method of Ref. 1 is not well founded in theory, since the 'three-quarter-chord theorem,' developed initially for two-dimensional aerofoils, has been applied beyond the limits of its validity to estimate not only the effect of bound vortices of finite length but also the effect of trailing vortices at many spanwise positions. The method cannot be used to predict the chordwise loading. It is applicable only to thin wings and cannot predict the pressure distribution. Similarly the effect of camber cannot be taken into account. Finally, the calculation is much longer and more cumbersome than the one described in this report.

The present method, which is based on the approach to swept wing problems described in Refs. 5 and 11, can provide the spanwise and chordwise loading and the pressure distribution on a cranked wing in incompressible flow. The calculation can be performed quite rapidly, even for 31 spanwise pivotal points. It can readily be extended to cambered aerofoil sections (Ref. 7). Hunn[9] has shown recently how the spanwise loading calculation method presented in Ref. 5 and followed in the present report can be extended to the case of elastic wings. Since cranked plan-forms may be contemplated primarily because of aeroelastic considerations, this last feature is an important advantage.

NOTATION

a		Sectional lift slope, C_L/α_e
a_0		Two-dimensional lift slope, C_L/α_{e0}
c		Local chord
f		Camber, in terms of the chord
$f(\varphi)$		A function of sweep which appears in the expressions for the velocities near a crank or kink
h		Chordwise distance of the local aerodynamic centre from the leading edge
Δh		Chordwise distance of the local aerodynamic centre from the quarter-chord point
k		Reduction factor to the lift slope due to the boundary layer
m		Chordwise loading parameter due to camber
n		Chordwise loading parameter due to incidence
n_0	=	n near the centre or tip of a wing of very large aspect ratio
$n_0{}^*$	=	n near the crank of a wing of very large aspect ratio
$n_0{}'$	=	n on a finite wing for which low aspect ratio effects need not be considered
$q(x)$		Chordwise source distribution (strength per unit area) to represent wing thickness

NOTATION—*continued.*

$q^*(X)$	Source distribution along X-axis at the crank of a wing
t/c	Thickness/chord ratio
v_x, v_y, v_z / v_X, v_Y	Velocity increments along the x, y, z, X and Y axes respectively
x, y, z	Rectangular axes : x in direction of free steam, y spanwise to starboard and z vertically downwards : co-ordinates non-dimensional with the chord
A	Aspect ratio
$C(m)$	A function of m plotted in Ref. 7
$C_p(x)$	Pressure coefficient $= p - p_0/\frac{1}{2}\rho V_0^2$
$\Delta C_p(x)$	Chordwise loading = difference of C_p on the two wing surfaces
C_L	Sectional lift coefficient
$\bar{C}_L$	Overall lift coefficient
C_{Di}	Sectional induced drag coefficient
$\bar{C}_{Di}$	Overall induced drag coefficient
K_i	Induced drag factor $= \bar{C}_{Di} \Big/ \frac{C_L^2}{\pi A}$
C_N	Normal force coefficient
E	Source strength per unit length $= q(x) \cos\varphi \, . \, dx$
$S_v^{(1)}, S_v^{(2)}, S_v^{(3)}, S_v^{(4)}$	Functions of the wing profile
V	Total velocity at a point $= \sqrt{\{(V_0 + v_x)^2 + v_y^2 + v_z^2\}}$
V_0	Free-stream velocity
X, Y	Rectangular axes : X in direction perpendicular to the line of sweep, Y parallel to the line of sweep : co-ordinates non-dimensional with the chord
α	Geometric incidence
α_e	Effective incidence
α_{e0}	Effective incidence of an infinite wing
$\Delta\alpha$	Equivalent incidence due to camber
$\gamma(x)$	Chordwise distribution of vorticity representing lifting effect of wing
η	Non-dimensional spanwise co-ordinate $= y \, . \, c/\frac{1}{2}b$
$\lambda = \lambda(y)$	Spanwise interpolation function
φ	Angle of sweep (usually of mid-chord line)
$\varphi^* =$	$\tan^{-1} \frac{1}{2}(\tan\varphi_o - \tan\varphi_i)$
φ_V	Mean sweep angle of the vorticity vectors
φ_m	Mean sweep angle of complete wing
φ_e	Effective sweep
ω	Induced downwash factor

NOTATION—*continued.*

Suffixes

x, y, z, X, Y	In the x, y, z, X and Y directions respectively
c, T, cr.	At the centre, tip and crank of a wing, respectively
s	At the sheared part of a wing
a	Due to incidence
f	Due to camber
$\left.\begin{matrix} r \\ n \end{matrix}\right\}$	Indicating chordwise and spanwise pivotal points
i	Referring to the inboard side of a crank
o	Referring to the outboard side of a crank
0	Referring to an infinite wing or Referring to the free stream
U.S., L.S.	Upper surface, lower surface respectively

REFERENCES

No.	*Author*	*Title, etc.*
1	F. W. Diederich and W. O. Latham ..	Calculated aerodynamic loadings of M, W and A wings in incompressible flow. N.A.C.A. RM.L51E29. August, 1951.
2	G. S. Campbell	A finite-step method for the calculation of span loadings of unusual plan-forms. N.A.C.A. RM.L50L13. July, 1951.
3	V. M. Falkner	The solution of lifting plane problems by vortex-lattice theory. R. & M. 2591. September, 1947.
4	H. Multhopp	Die Berechnung der Auftriebsverteilung von Tragflügeln. *Luftfahrtforschung*, Vol. 15, 1938, p. 153. Translated in A.R.C. 8516.
5	D. Küchemann	A simple method for calculating the span and chordwise loadings on thin swept wings. R.A.E. Report Aero. 2392. A.R.C. 13,758. (Unpublished.)
6	D. Küchemann	A simple method for calculating the span and chordwise loadings on straight and swept wings of any given aspect ratio at subsonic speeds. R. & M. 2935. August, 1952.
7	G. G. Brebner	The application of camber and twist to swept wings in incompressible flow. C.P. 171. March, 1952.
8	J. Weber, D. A. Kirby and D. J. Kettle	An extension of Multhopp's method of calculating the spanwise loading of wing fuselage combinations. R. & M. 2872. November, 1951.
9	B. A. Hunn	A method of estimating the loading on an elastic airframe. *J. R. Ae. Soc.*, Vol. 56, p. 261. April, 1952.
10	D. Küchemann	Wing junction, fuselage and nacelles for swept-back wings. R.A.E. Report Aero. 2219. A.R.C. 11,035. (Unpublished.) (Some material from this is contained in R. & M. 2908. March, 1953.)

REFERENCES—*continued.*

No.	*Author*	*Title, etc.*
11	J. Weber	A simple method for calculating the chordwise pressure distribution on two-dimensional and swept wings for aerofoil sections of finite thickness. R.A.E. Report Aero. 2391. A.R.C. 13,757. (Unpublished.) (This has since been replaced by a much more comprehensive paper published as R. & M. 2918. July, 1953.)
12	G. G. Brebner and J. A. Bagley ..	Pressure and boundary-layer measurements on a two-dimensional wing at low speed. R. & M. 2886. February, 1952.
13	J. Weber and G. G. Brebner	Low-speed tests on 45-deg swept-back wings. Part I : Pressure measurements on wings of aspect ratio 5. R. & M. 2882. May, 1951.
14	D. Küchemann, J. Weber and G. G. Brebner.	Low-speed tests on wings of 45-deg sweep. Part II : Balance and pressure measurements on wings of different aspect ratios. R. & M. 2882. May, 1951.
15	D. Küchemann	Some methods of determining the effect of the boundary layer on the lift slope of straight and swept wings. R.A.E. Tech. Note Aero. 2167. A.R.C. 15,245. (Unpublished.)
16	R. W. Herr	Preliminary experimental investigation of flutter characteristics of M and W wings, N.A.C.A. RM.L51E31. August, 1951.
17	U. R. Barnett and R. H. Lange ..	Low-speed pressure-distribution measurements at a Reynolds number of $3{\cdot}5 \times 10^6$ on a wing with leading-edge sweep-back decreasing from 45 deg at the root to 20 deg at the tip. N.A.C.A. RM.L50A23a. July, 1950.
18	S. Neumark	Velocity distribution on straight and swept-back wings of small thickness and infinite aspect ratio at zero incidence. R. & M. 2713. May, 1947.
19	R. T. Jones	Subsonic flow over thin oblique airfoils at zero lift. N.A.C.A. Tech. Note 1340. June, 1947.
20	F. Ursell	Notes on the linear theory of incompressible flow round symmetrical swept-back wings at zero lift. *Aero. Quart.*, Vol. 1, p. 101. May, 1949.

TABLE 1

Pressure and Normal Force Coefficients at the crank of Wing I (Fig. 2b)

C_p

	$\frac{x}{c}$	α (deg)										
		−2·2	−1·1	0	1·1	2·2	3·3	4·4	5·5	6·6	8·8	11·1
UPPER SURFACE	0·95	0·117	0·122	0·120	0·121	0·120	0·121	0·121	0·115	0·082	0·054	−0·090
	0·85	0·064	0·062	0·058	0·058	0·057	0·057	0·057	0·055	0·055	0·024	−0·113
	0·75	0·027	0·022	0·016	0·011	0·006	0·001	−0·001	−0·004	−0·001	−0·011	−0·109
	0·65	−0·033	−0·044	−0·053	−0·058	−0·067	−0·074	−0·077	−0·079	−0·078	−0·071	−0·115
	0·50	−0·109	−0·125	−0·142	−0·157	−0·174	−0·191	−0·204	−0·215	−0·222	−0·221	−0·197
	0·35	−0·214	−0·245	−0·288	−0·304	−0·333	−0·362	−0·387	−0·413	−0·436	−0·464	−0·450
	0·225	−0·263	−0·311	−0·363	−0·419	−0·468	−0·523	−0·566	−0·621	−0·663	−0·743	−0·800
	0·15	−0·256	−0·322	−0·396	−0·472	−0·548	−0·629	−0·686	−0·757	−0·833	−0·977	−1·076
	0·08	−0·186	−0·294	−0·414	−0·536	−0·646	−0·788	−0·837	−0·969	−1·070	−1·359	−1·587
	0·03	−0·001	−0·184	−0·390	−0·609	−0·834	−1·153	−1·321	−1·624	−1·875	−2·470	−2·964
	0·01	0·309	0·034	−0·292	−0·658	−1·044	−1·467	−1·835	−2·516	−3·027	−4·288	−5·342
	0	—	—	0·990	0·992	0·994	0·692	0·058	−0·604	−1·913	−3·562	−6·047
LOWER SURFACE	0·01	−1·002	−0·599	−0·229	0·096	0·373	0·615	0·780	0·902	0·969	0·941	0·754
	0·03	−0·834	−0·567	−0·347	−0·142	0·043	0·226	0·374	0·502	0·622	0·793	0·900
	0·08	−0·629	−0·507	−0·389	−0·273	−0·166	−0·055	0·040	0·135	0·221	0·388	0·527
	0·15	−0·520	−0·452	−0·377	−0·303	−0·232	−0·158	−0·093	−0·030	0·033	0·159	0·269
	0·225	−0·450	−0·400	−0·349	−0·296	−0·245	−0·191	−0·144	−0·099	−0·051	0·044	0·134
	0·35	−0·328	−0·298	−0·281	−0·243	−0·210	−0·174	−0·145	−0·117	−0·086	−0·025	0·033
	0·50	−0·169	−0·150	−0·131	−0·118	−0·100	−0·103	−0·078	−0·057	−0·039	−0·006	0·029
	0·65	−0·056	−0·044	−0·036	−0·026	−0·015	−0·006	−0·003	0·005	0·012	0·027	0·044
	0·75	0·003	0·011	0·012	0·019	0·024	0·029	0·036	0·037	0·038	0·044	0·047
	0·85	0·058	0·059	0·059	0·064	0·065	0·068	0·069	0·066	0·066	0·058	0·047
	0·95	0·120	0·121	0·120	0·120	0·117	0·118	0·114	0·107	0·099	0·073	0·038
		C_N										
		−0·149	−0·080	0	0·077	0·154	0·232	0·289	0·364	0·425	0·556	0·703

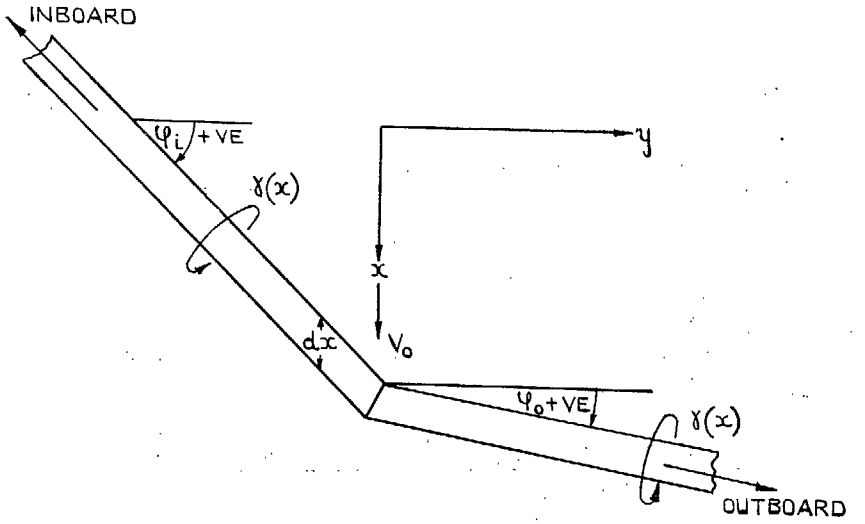

FIG. 1a. Cranked vortex filament.

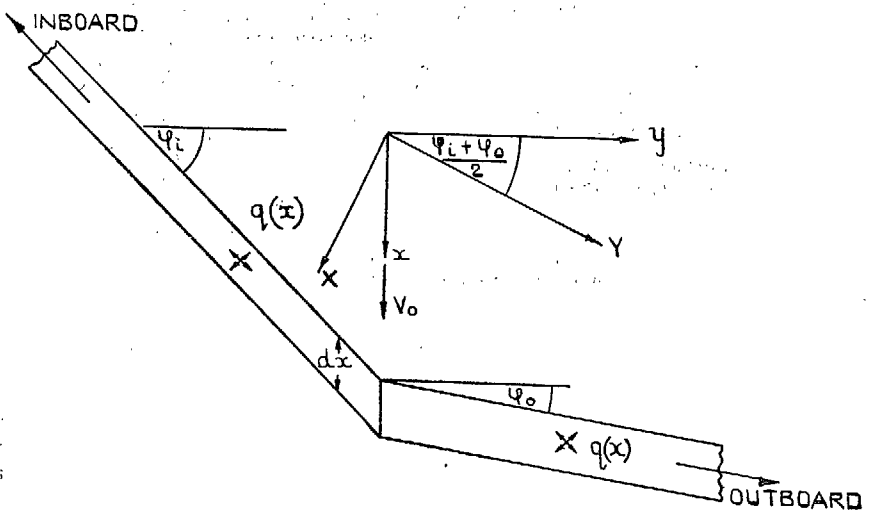

FIG. 1b. Cranked source line.

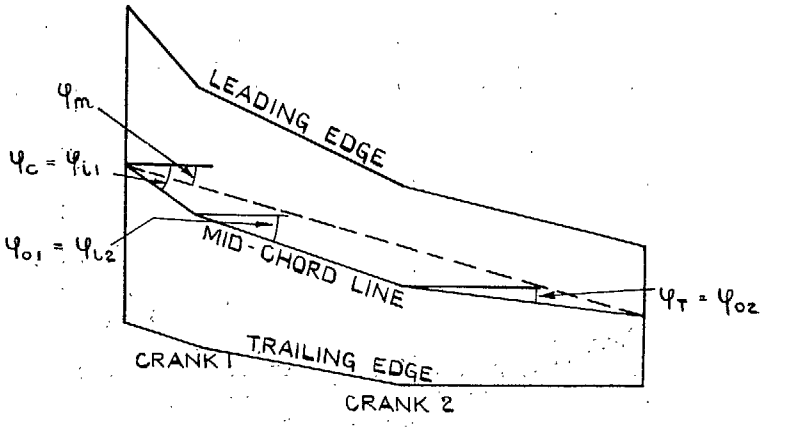

FIG. 2a. Definitions of sweep angles used in calculations.

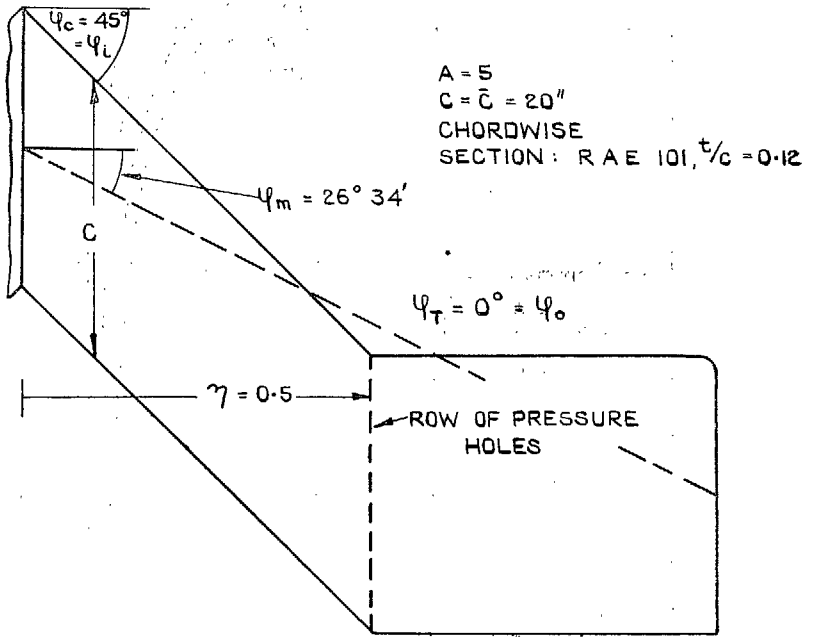

FIG. 2b. Plan-form of cranked wing tested (Wing I).

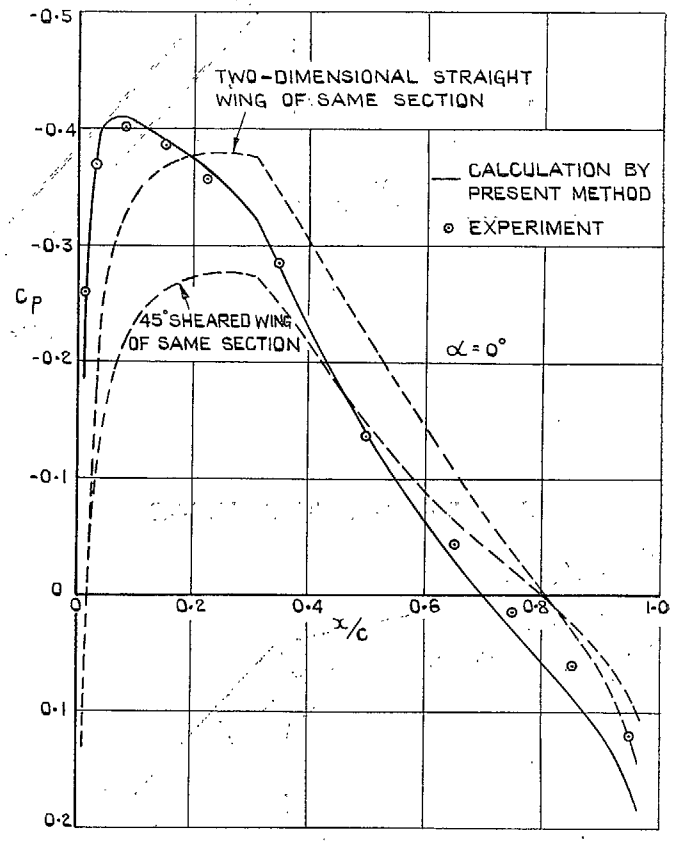

FIG. 3. Experimental and calculated chordwise pressure distribution at zero incidence at the crank of Wing I.

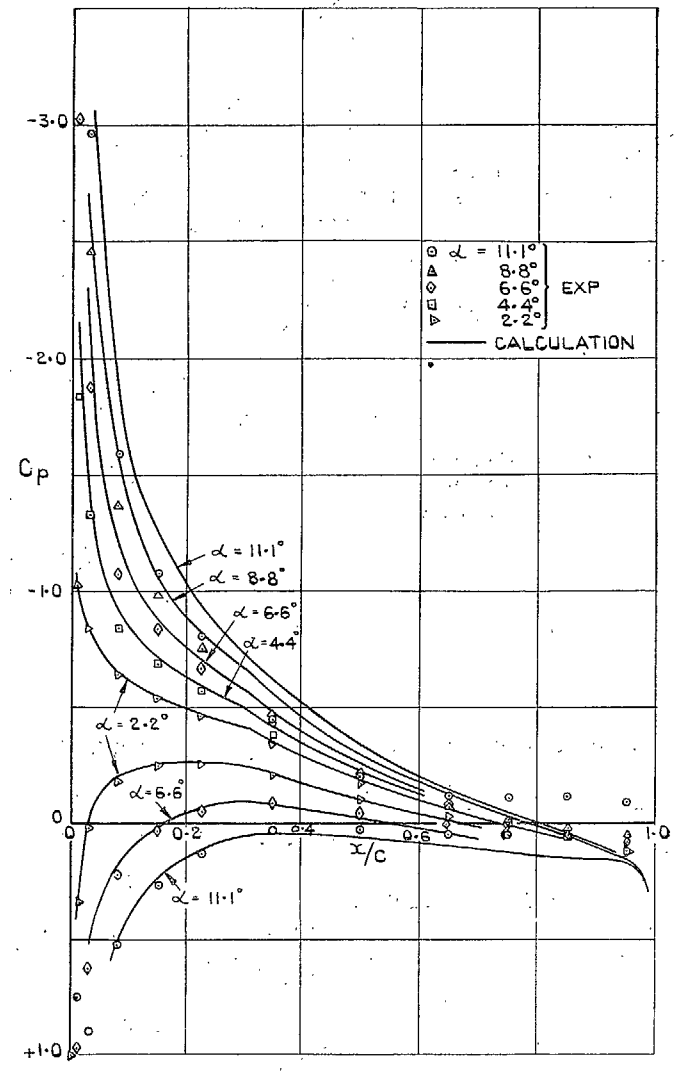

FIG. 4. Experimental and calculated chordwise pressure distributions at incidences up to 11·1 deg at the crank of Wing I.

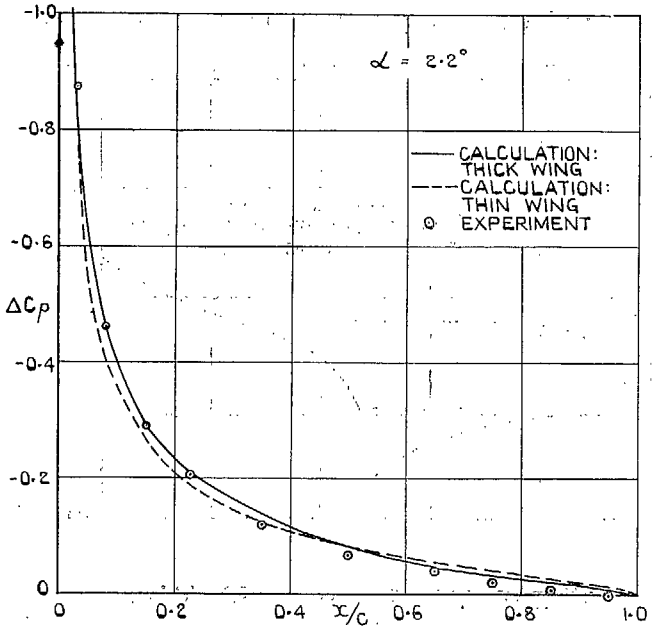

FIG. 5. Chordwise loading at the crank of Wing I: $\alpha = 2{\cdot}2$ deg.

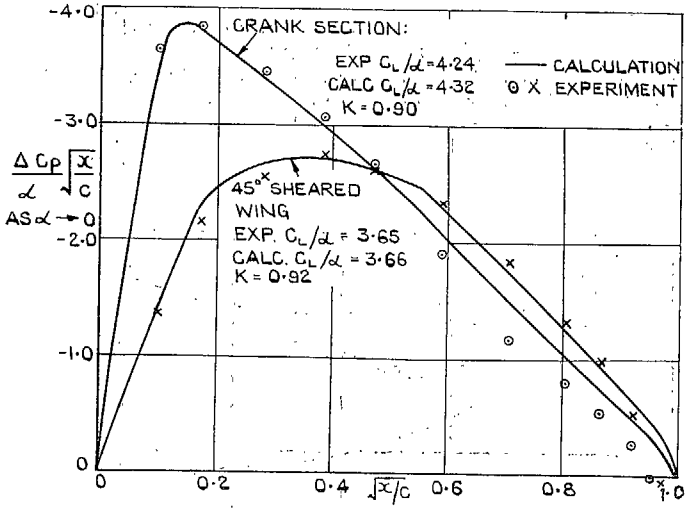

FIG. 6. Chordwise loading at the crank of Wing I: $\alpha \to 0$ deg.

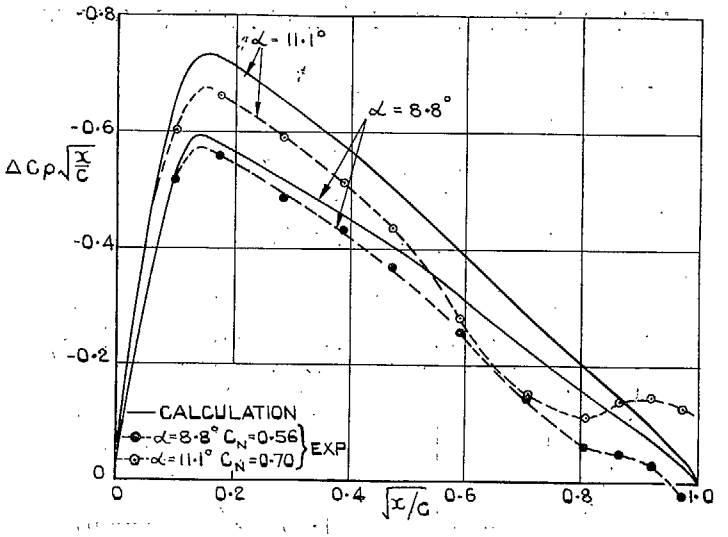

FIG. 7. Chordwise loadings at the crank of Wing I: $\alpha = 8{\cdot}8$ deg and $\alpha = 11{\cdot}1$ deg.

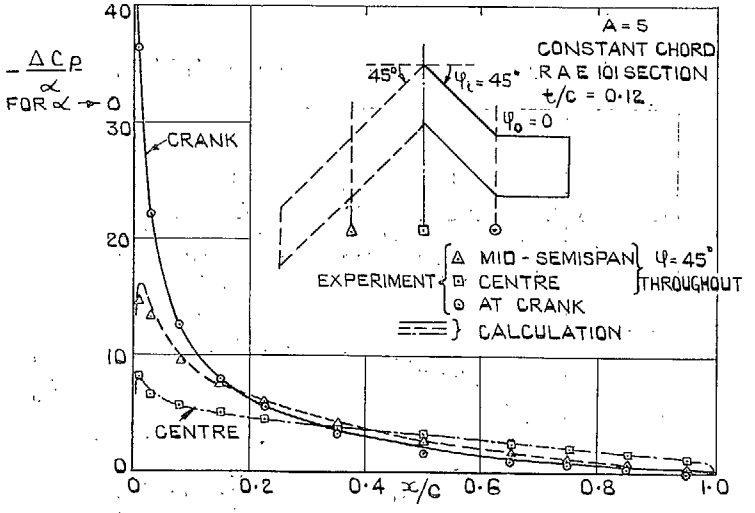

FIG. 8. Comparison of chordwise loadings on a fully swept wing and a cranked wing (Wing I): $\alpha \to 0$ deg.

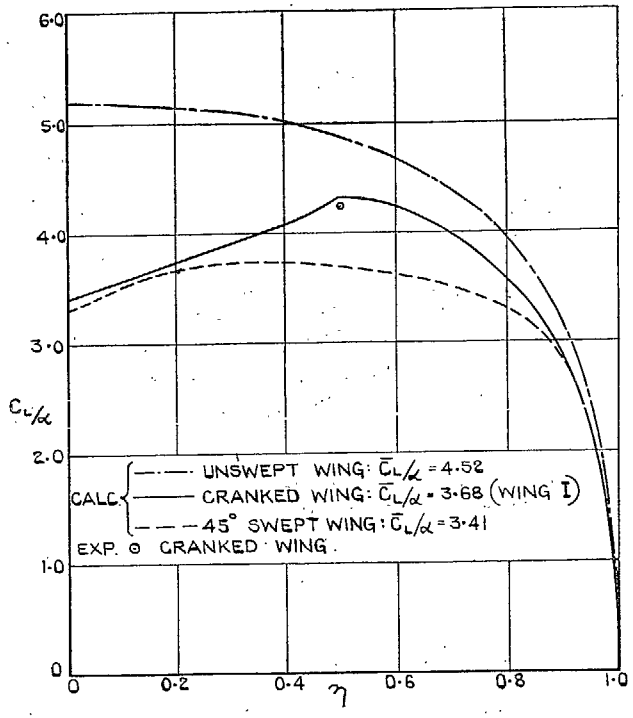

FIG. 9. Comparison of spanwise loadings.

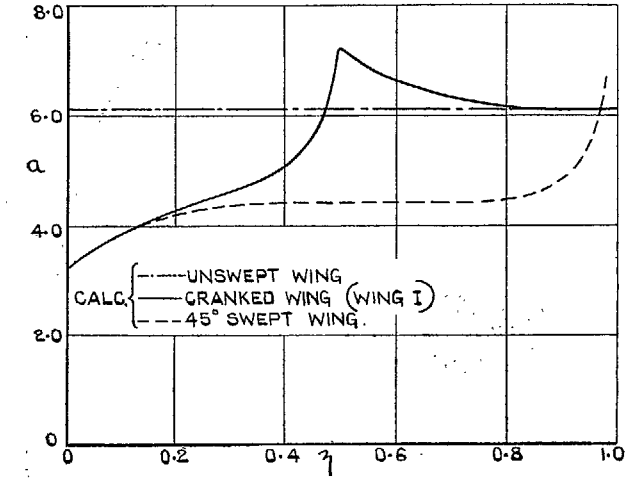

FIG. 10. Comparison of local lift slopes.

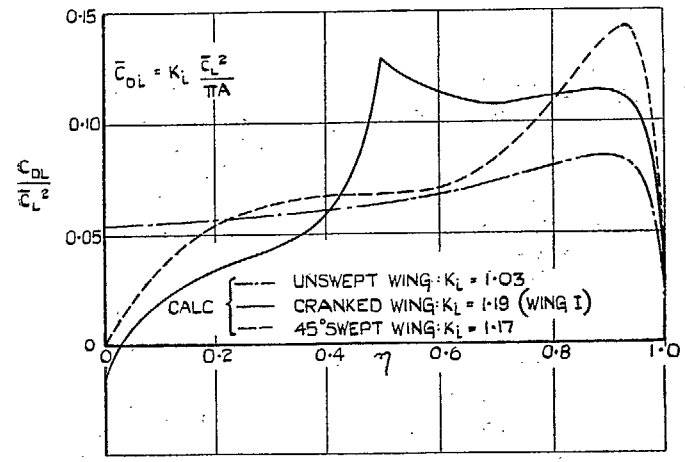

FIG. 11. Comparison of local induced drag.

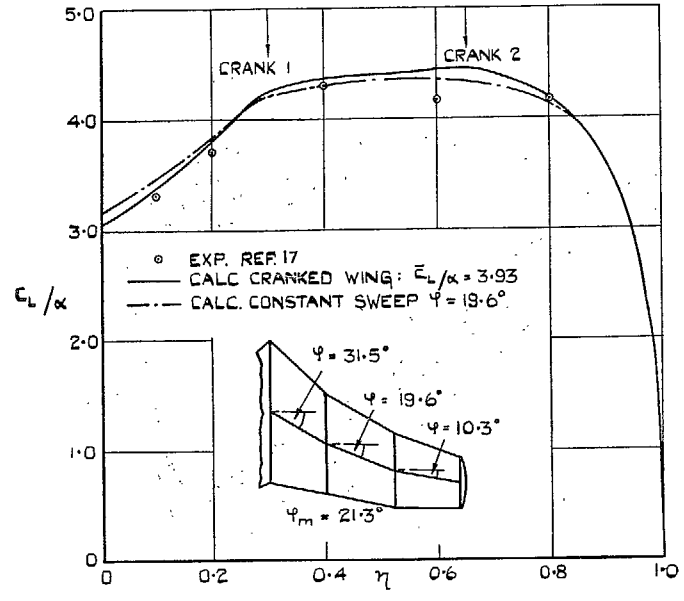

FIG. 12. Spanwise loading of a cranked wing. Ref. 17.

J4332 Wt.18/9296 K7 10/55 D&Co. 34/263

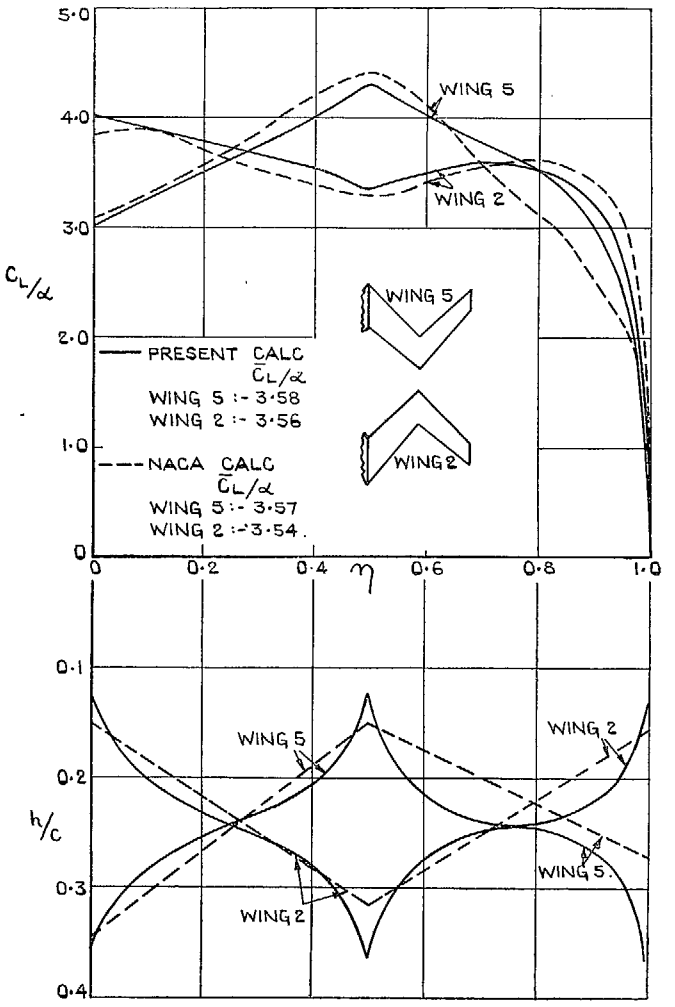

FIG. 13. Spanwise loading and aerodynamic centre : Wings 2 and 5. Ref. 1.

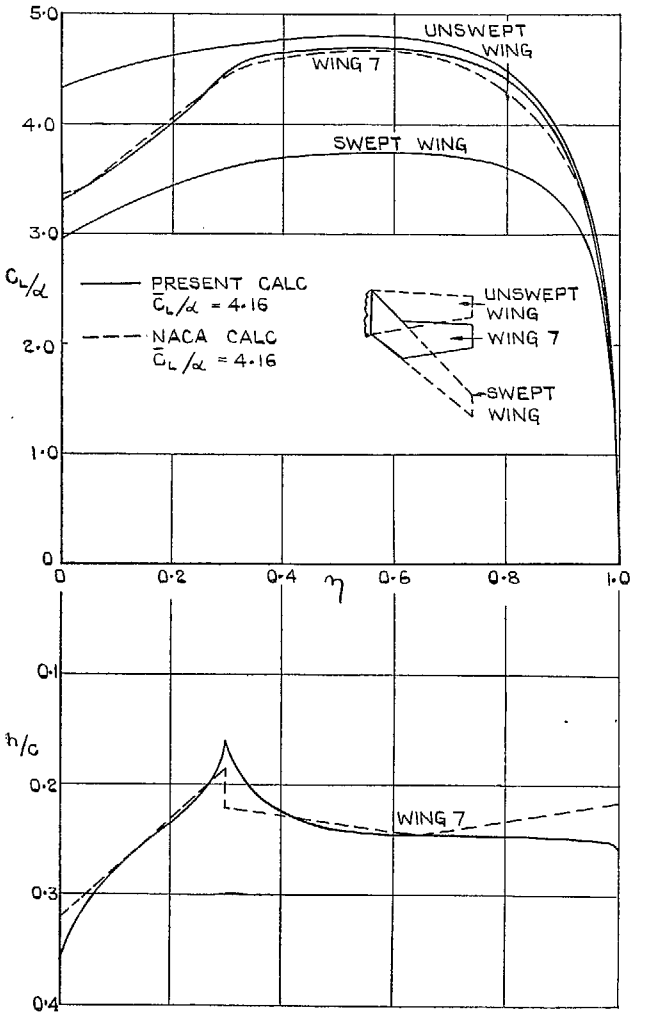

FIG. 14. Spanwise loading and aerodynamic centre : Wing 7. Ref. 1.

PRINTED IN GREAT BRITAIN

Publications of the Aeronautical Research Council

ANNUAL TECHNICAL REPORTS OF THE AERONAUTICAL RESEARCH COUNCIL (BOUND VOLUMES)

1938 Vol. I. Aerodynamics General, Performance, Airscrews. 50*s.* (51*s.* 2*d.*)
Vol. II. Stability and Control, Flutter, Structures, Seaplanes, Wind Tunnels, Materials. 30*s.* (31*s.* 2*d.*)

1939 Vol. I. Aerodynamics General, Performance, Airscrews, Engines. 50*s.* (51*s.* 2*d.*)
Vol. II. Stability and Control, Flutter and Vibration, Instruments, Structures, Seaplanes, etc. 63*s.* (64*s.* 2*d.*)

1940 Aero and Hydrodynamics, Aerofoils, Airscrews, Engines, Flutter, Icing, Stability and Control, Structures, and a miscellaneous section. 50*s.* (51*s.* 2*d.*)

1941 Aero and Hydrodynamics, Aerofoils, Airscrews, Engines, Flutter, Stability and Control, Structures. 63*s.* (64*s.* 2*d.*)

1942 Vol. I. Aero and Hydrodynamics, Aerofoils, Airscrews, Engines. 75*s.* (76*s.* 3*d.*)
Vol. II. Noise, Parachutes, Stability and Control, Structures, Vibration, Wind Tunnels. 47*s.* 6*d.* (48*s.* 8*d.*)

1943 Vol. I. Aerodynamics, Aerofoils, Airscrews. 80*s.* (81*s.* 4*d.*)
Vol. II. Engines, Flutter, Materials, Parachutes, Performance, Stability and Control, Structures. 90*s.* (91*s.* 6*d.*)

1944 Vol. I. Aero and Hydrodynamics, Aerofoils, Aircraft, Airscrews, Controls. 84*s.* (85*s.* 8*d.*)
Vol. II. Flutter and Vibration, Materials, Miscellaneous, Navigation, Parachutes, Performance, Plates and Panels, Stability, Structures, Test Equipment, Wind Tunnels. 84*s.* (85*s.* 8*d.*)

ANNUAL REPORTS OF THE AERONAUTICAL RESEARCH COUNCIL—

1933–34	1*s.* 6*d.* (1*s.* 8*d.*)	1937	2*s.* (2*s.* 2*d.*)
1934–35	1*s.* 6*d.* (1*s.* 8*d.*)	1938	1*s.* 6*d.* (1*s.* 8*d.*)
April 1, 1935 to Dec. 31, 1936	4*s.* (4*s.* 4*d.*)	1939–48	3*s.* (3*s.* 2*d.*)

INDEX TO ALL REPORTS AND MEMORANDA PUBLISHED IN THE ANNUAL TECHNICAL REPORTS, AND SEPARATELY—

April, 1950 – – – – – R. & M. No. 2600. 2*s.* 6*d.* (2*s.* 7½*d.*)

AUTHOR INDEX TO ALL REPORTS AND MEMORANDA OF THE AERONAUTICAL RESEARCH COUNCIL—

1909–January, 1954 – – – R. & M. No. 2570. 15*s.* (15*s.* 4*d.*)

INDEXES TO THE TECHNICAL REPORTS OF THE AERONAUTICAL RESEARCH COUNCIL—

December 1, 1936 — June 30, 1939.	R. & M. No. 1850.	1*s.* 3*d.* (1*s.* 4½*d.*)
July 1, 1939 — June 30, 1945. –	R. & M. No. 1950.	1*s.* (1*s.* 1½*d.*)
July 1, 1945 — June 30, 1946. –	R. & M. No. 2050.	1*s.* (1*s.* 1½*d.*)
July 1, 1946 — December 31, 1946.	R. & M. No. 2150.	1*s.* 3*d.* (1*s.* 4½*d.*)
January 1, 1947 — June 30, 1947. –	R. & M. No. 2250.	1*s.* 3*d.* (1*s.* 4½*d.*)

PUBLISHED REPORTS AND MEMORANDA OF THE AERONAUTICAL RESEARCH COUNCIL—

Between Nos. 2251–2349. – –	R. & M. No. 2350.	1*s.* 9*d.* (1*s.* 10½*d.*)
Between Nos. 2351–2449. – –	R. & M. No. 2450.	2*s.* (2*s.* 1½*d.*)
Between Nos. 2451–2549. – –	R. & M. No. 2550.	2*s.* 6*d.* (2*s.* 7½*d.*)
Between Nos. 2551–2649. – –	R. & M. No. 2650.	2*s.* 6*d.* (2*s.* 7½*d.*)

Prices in brackets include postage

HER MAJESTY'S STATIONERY OFFICE

York House, Kingsway, London W.C.2; 423 Oxford Street, London W.1 (Post Orders: P.O. Box 569, London S.E.1); 13a Castle Street, Edinburgh 2; 39 King Street, Manchester 2; 2 Edmund Street, Birmingham 3; 109 St. Mary Street, Cardiff; Tower Lane, Bristol 1; 80 Chichester Street, Belfast, *or through any bookseller*

S.O. Code No. 23-2947